Flight Mechanical Modeling of a Precision Guided Mortar Munition

JOHN W.C. ROBINSON

FOI, Swedish Defence Research Agency, is a mainly assignment-funded agency under the Ministry of Defence. The core activities are research, method and technology development, as well as studies conducted in the interests of Swedish defence and the safety and security of society. The organisation employs approximately 1000 personnel of whom about 800 are scientists. This makes FOI Sweden's largest research institute. FOI gives its customers access to leading-edge expertise in a large number of fields such as security policy studies, defence and security related analyses, the assessment of various types of threat, systems for control and management of crises, protection against and management of hazardous substances, IT security and the potential offered by new sensors.

FOI
Defence Research Agency
Defence and Security,
Systems and Technology
SE-164 90 Stockholm

Phone: +46 8 555 030 00
Fax: +46 8 555 031 00

www.foi.se

FOI-R--2618--SE Technical report
ISSN 1650-1942 July 2010

Defence and Security, Systems and Technology

John W.C. Robinson

Flight Mechanical Modeling of a Precision Guided Mortar Munition

Titel	Flygmekanisk modell av en precisionsstyrd artillerigranat
Title	Flight Mechanical Modeling of a Precision Guided Mortar Munition
Rapportnummer / Report no	FOI-R--2618--SE
Rapporttyp / Report type	Teknisk rapport / Technical report
Utgivningsår / Year	2010
Antal sidor / Pages	64
Kund / Customer	Swedish Armed Forces
Forskningsområde	5. Bekämpning och skydd
Research area	5. Strike and Protection
Delområde	51. Vapen och skydd
Sub area code	51. Weapons and Protection
Projektnummer / Project no	E20674
Godkänd av / Approved by	Nils Olsson Head, Defence and Security, Systems and Technology
ISSN	ISSN-1650-1942

FOI Swedish Defence Research Agency
Defence and Security, Systems and Technology
SE-164 90 STOCKHOLM

Abstract

The report describes the development of a performance model for a precision guided mortar munition (PGMM) with deployable wings. Most of the material, however, is generally applicable to missiles with essentially cylinder symmetric configuration which are operated in skid-to-turn mode. Topics covered are modeling of aerodynamic and flight mechanical characteristics using so called handbook methods, and performance attainable with a simple linear controller. Particular attention is devoted to development of a reduced dynamics model based on two sets of linearized pitch plane dynamics, and the assumptions and simplifications that are made in this process. The vehicle used as design example (PGMM) is a subsonic glider with moderate turn performance and relatively low glide ratio where the goal of the aerodynamic design is primarily to enhance range (compared to ballistic flight) and add maneuvering capabilities to hit slowly moving targets.

Keywords

Flight Mechanics, Control, Aerodynamics, Guided Munition, Missile

Sammanfattning

Rapporten beskriver utvecklingen av en prestandamodell för en precisionsstyrd granatkastargranat (PGMM) med utfällbara vingar. Det mesta av materialet är emellertid generellt tillämpbart på missiler med väsentligen cylindersymmetrisk konfiguration som flygs enligt den s.k. “skid-to-turn”-principen. Ämnen som behandlas är modellering av aerodynamiska och flygmekaniska egenskaper med hjälp av s.k. handboksmetoder, samt uppnåeliga prestanda med en enkel linjär regulator. Speciell uppmärksamhet ägnas åt utveckling av en reducerad dynamisk modell baserad på två uppsättningar av den linjäriserade tippkanalsdynamiken, och de antaganden och förenklingar som görs i denna process. Farkosten som används som designexempel (PGMM) är en subsonisk glidfarkost med modesta svängprestanda och relativt lågt glidtal. Det främsta målet med den aerodynamiska utformningen i detta fall är att utöka räckvidden (jämfört med ballistisk flykt) och tillföra manöveregenskaper för att slå fordon och andra långsamt rörliga mål.

Nyckelord

Flygmekanik, Styrning, Aerodynamik, Styrd Granat, Missil, Robot

Contents

1 Introduction

This work concerns performance modeling of a missile in the form of a precision guided mortar munition (PGMM). However, the methods and results are generally applicable to a large class of (essentially cylinder symmetric) missiles. The PGMM has deployable wings for increased range and maneuverability, and the flight mechanic (and aerodynamic) characteristics are therefore similar to a missile in non-powered flight. Our goal is to derive a performance model which can be used to evaluate different design and operational concepts, such as seeker design and flight and maneuver strategies in various types of missions.

In order to analytically describe the motion of a missile one needs equations describing the dynamics and we shall rely on various forms of equations derived from Newton-Euler's (NE) rigid body equations. In the NE equations the forces and moments can be interpreted as "driving terms" and for a missile in atmospheric operation these are caused by gravity, thrust and aerodynamics. Therefore, we shall first deal with aerodynamic modeling and then proceed to modeling of the rigid body dynamics when developing our performance modeling tools. It is assumed that the reader has some familiarity with basic flight mechanics and aerodynamic concepts, such as Newton-Euler's rigid body equations and aerodynamic force and moment coefficients (Stevens & Lewis, 2003).

1.1 Modeling Missile Aerodynamics

The two most important pieces of information for performance assessment of a missile in non-powered atmospheric flight are the lift and drag curves. The lift curve gives turning performance, and for a missile which is also supposed to glide (like the mortar round with wings we shall consider) it gives also part of the information to determine the attainable range. The other part of the information needed to determine attainable range is the drag curve, and it moreover gives information about the energy "bleed" during maneuvering. Fortunately, both of these curves can often be easily calculated, to a good approximation, using so called handbook methods (Fleeman, 2006). This is especially true for (slender) cylinder symmetric missiles with simple configurations in terms of wings and control surfaces. Aerodynamic handbook methods combine formulas derived from various theories (slender body theory, linear wing theory, Newtonian impact theory) with empirical corrections and have proven very successful in predicting missile performance when compared to wind tunnel tests for such simple configurations (Abney & McDaniel, 2005; Sooy & Schmidt, 2005; Simon & Blake, 1999; Lesieutre *et al.*, 1996). After having described the PGMM configuration in Chapter 2, we shall use such handbook methods in Chapter 3 to make the aerodynamic predictions needed for the work in Chapter 4 where we develop a reduced "2+3-DOF" model of the dynamics for the PGMM.

1.2 Modeling Missile Flight Mechanics

The goal with development of a performance model for a missile or guided projectile is to provide a simplified description of its dynamics which has enough detail to provide *accurate predictions in the intended evaluation scenarios,* but not more than this.[1] This can often be translated to mean that the dynamics

[1] Albert Einstein is attributed to having said "Things should be made as simple as possible, but not simpler."

should be modeled accurately enough to represent the behavior as it appears to an outside observer. For instance, an outside observer can in general not discern the part of the dynamics of a guided missile that is directly related to the motion of the actuators (e.g. the servos driving the control surfaces) since this occurs on a much faster time scale than the overall motion of the missile airframe. Moreover, to an outside observer it might not be relevant to single out the the parts of the overall dynamics that are related to the control system, sensors or signal processing, even if they contribute to the dynamics on the same timescale as the airframe dynamics. Indeed, it is often the goal of the control system to make certain dynamic properties invariant with respect to parameter variations (such as changes in center-of-mass, airspeed and altitude, or even angle of attack) via *dynamics synthesis* and therefore it is not relevant to try to describe e.g. the bare airframe dynamics separately in the final model. Furthermore, in studies of homing missile systems the (controlled) missile airframe dynamics and guidance dynamics are often lumped together ("the homing loop dynamics") (Zarchan, 1994). A performance model will therefore normally include most, or all of, these parts of the dynamics, described on a simplified form.

1.2.1 The simplest models

It follows from the discussion above that a good performance model can often be obtained by reducing the detailed dynamics to a form which captures the behavior of the vehicle as it appears from a distance to an observer with *limited resolution in time and space*. The most extreme example of this is an observer who views the missile as a point mass, and therefore is only interested in the motion of the center of mass (CoM). This gives a *three degrees-of-freedom* (3-DOF) model, which is one of the most often used simplified descriptions of a missile or projectile.

If one regards the missile as a rigid body and wants to account for the motion around the CoM there are several ways to proceed from the extreme 3-DOF case. One of the easiest ways is to restrict motion in space (in an Earth fixed reference frame) to lie in a plane, and study the motion around the CoM restricted to this plane. This approach leads to a 4-DOF model, where two degrees of freedom are used to describe the (translational) motion of the CoM in terms of the location coordinates and two degrees of freedom are used to describe the (rotational) motion around the CoM in terms of the pitch and roll angle. If the missile can be regarded as essentially cylinder symmetric (with regard to aerodynamic and mass configuration properties), which is often the case as a first approximation, one degree of freedom (roll angle) drops out, and the model can be reduced to 3-DOF (in the given plane in space). Such a model can be used to assess e.g. dynamic turn performance, i.e. how well a missile will be able to go in and out of a horizontal turn, or to assess the performance of engaging in a pitch-up or pitch-over, in case of a vertical maneuver.

In the case of a 3-DOF model of the latter type, where roll motion is disregarded, there is still a need for six state variables in the differential equation for the model. This is a consequence of the fact that the forces (described by a two-dimensional vector) determine the acceleration of CoM, which after two integrations affect the location of CoM (a two-dimensional vector), and the pitch moment (a scalar) determines the pitch acceleration, which after two integrations affects the pitch angle.[2]

[2]Thus, it is important to distinguish between the number of states and degrees of freedom. The degrees of freedom correspond to the minimal number of physical location variables that

1.2.2 Models of reduced complexity

If, on the other hand, one wants a model with high fidelity but possibly reduced complexity, compared to a full 12-state model (see below), a natural approach is to start with the full model and then remove states which are unnecessary (or uninteresting). For missiles which are essentially cylinder symmetric this often means that one in the body equations (see below) disregards the dynamics for the roll motion along the main axis, i.e. assumes that the angular velocity around this axis is zero. This reduces the number of state variables but the number of degrees of freedom is normally left at 6 (even though this results in a redundant parameterization of the dynamics[3]). However, since the most interesting variables for a maneuvering missile are those that correspond to velocities and angular velocities one could also consider these variables as representing the *essential* degrees of freedom (i.e. we consider the velocity level as the base for our model). Moreover, the dynamics for these variables (which are given by aerodynamics and gravity, and possibly propulsion) are considerably more complicated than those for the location variables: The location variables are obtained by integration of the velocity variables and therefore require no special modeling. A missile model with zero angular velocity around the main axis in the body equations could then be called (with a slight abuse of the standard language) a "2+3-DOF" model, and we shall henceforth use this terminology.

The "2+3-DOF" type of model just outlined normally employs 11 states and it is often convenient to express only some of these with respect to the Earth fixed frame which is implicit in all of the discussion above. In fact, the rotational part of the dynamics is most conveniently described in terms of a body fixed Cartesian coordinate system since the moment of inertia matrix then becomes time invariant, if one neglects mass flow effects (e.g. due to propulsion). Moreover, it turns out that it is convenient to refer also the velocities to the body fixed system, partly because the aerodynamic forces are naturally expressed in the body fixed system. Only the location variables for CoM and the variables describing the orientation of the body fixed frame in the Earth fixed frame are then expressed with respect to the Earth frame.

1.2.3 Relation to full rigid body dynamics models

A full rigid body model based on Newton-Euler's (NE) equations, i.e. a full 6-DOF model, has 12 states, where six states come from the NE equations, three states come from an equation for the orientation of the body frame expressed in the Earth frame (via e.g. a restricted quaternion or Euler angles) and three states come from the simple kinematic relationship between position and velocity in the Earth frame. It might then appear that a "2+3-DOF" model with 11 states is not much of a simplification over a full model. However, with proper choice of coordinates (i.e. aerodynamic angles) the "2+3-DOF" approach yields two systems of dynamics (one for pitch and one for yaw) which are in general

can be used when describing the position and orientation, and the states correspond to the minimal number of generalized coordinates that can be used when formulating the (restricted) dynamics (for the evolution of the position and orientation).

[3]Insisting that the angular velocity around the main axis is zero is a nonholonomic condition, i.e. a condition on the tangent vectors, not the base manifold. However, using the reduction techniques of Kane et al. (Kane & Wang, 1965; Kane & Lewinson, 1985) one can make a variable transformation and reduce the dimension of the base manifold to that of the restricted tangent space. Thus, the minimal degrees of freedom for zero roll rate is 5, the minimal number of state variables is 10, and the quotation marks around "2+3-DOF" can really be removed.

only weakly coupled, and linearization effectively *decouples* these systems into two sets of equations of *the same form*. Moreover, this form is preserved under linear state feedback, so a simple linear controller is easily included in the model.

In Chapter 4 we shall go through in detail how "2+3-DOF" models can be developed along these lines in a systematic way. The results are in no way new, they can be found (in different forms) in various places in the flight mechanics literature, but we present them here in collected form (as a "manual") and point out what assumptions and simplifications are introduced in each step of the derivation.

1.3 Notation

The notation used is standard; in the aerodynamics related parts we have tried to adhere to the notation most often used in the aerodynamics community and in the dynamics related parts we have used notation from the dynamics and control community. Thus, for example, vectors and matrices are denoted with bold face, such as $\boldsymbol{F}$, and vectors are generally considered to be column vectors unless otherwise noted. Transposition of a vector or matrix is marked as $\boldsymbol{F}^T$ and the norm (always the 2-norm) of a vector is marked as $\|\boldsymbol{F}\|$. The (one-dimensional) subspace spanned by a vector $\boldsymbol{v}$ is marked $[\boldsymbol{v}]$ and the orthogonal complement is denoted $[\boldsymbol{v}]^\perp$ (the base space in these contexts is always $\mathbb{R}^3$). The symbol $\boldsymbol{I}$ is reserved for the identity matrix in $\mathbb{R}^3$ and the projection operator (matrix) for projection onto e.g. a subspace $[\boldsymbol{v}]$ is denoted $\boldsymbol{P}_{[\boldsymbol{v}]}$.

1.4 Acknowledgements

The author wishes to extend his deep appreciation to Mr. F. Berefelt, FOI, for his thorough reading of the manuscript, and the comments and suggestion offered which helped to improve the presentation considerably. (Any remaining errors, mistakes or ambiguities are of course completely the responsibility of the author.)

2 Missile Configuration

The 120mm PGMM that we use as modeling example in this report is a conceptual design, with ideas borrowed from the Lockheed Martin/Diehl design XM395 (Bischer, 1999; Hollingsworth, 2002; Ness, 2004, p. 554), see Figure 2.1. Our version of the PGMM, depicted in Figure 2.2, differs from the Lockheed

Figure 2.1: The 120mm precision guided mortar munition round developed by Lockheed Martin/Diehl (Ness, 2004). (Source `www.globalsecurity.org`.)

Martin/Diehl design in several aspects, most notably in that ours has shorter wings (which fold backwards) and has a different internal layout, and therefore (presumably) a different mass distribution. The main advantage with the layout of our PGMM is that the warhead section is moved forward, which can give benefits for the effectiveness of certain types of warheads. The price paid

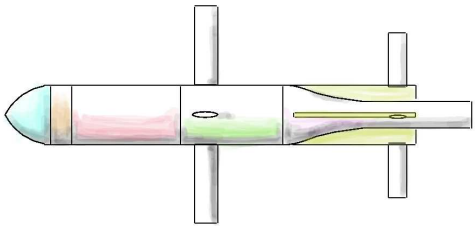

Figure 2.2: Outline of the (conceptual) 120mm PGMM modeled in this report (not drawn to scale). The four rectangular wings and tail fins are cruciform (and in the same planes), and the cylindrical body consists of five sections. Starting at the nose, the first section is the seeker lens assembly followed by the navigation electronics. The third section is the warhead and fuze, and the fourth section contains the battery and control electronics, and the four wings when they are folded (they deploy at apogee). The fifth section (boattail and tail tube) contains the servo actuators and linkages for the (movable) tail fins. Attached to the fifth section are four strakes which contain the tail fins when they are folded (they deploy immediately after the round has left the barrel).

is that the wings must be smaller since they cannot occupy space in the warhead section but must fold backwards into the battery and control electronics section. On the other hand, in our PGMM there are (small) strakes on the aft part of the body which adds some lifting surface area.[1]

2.1 Geometric Dimensions and Mass Distribution

The geometry for the lifting surfaces of the PGMM is given in Table 2.1, assuming a standard aircraft body coordinate system B (Stevens & Lewis, 2003, p. 72), and the mass distribution is given in Table 2.2. Since the nose tip hosts the seeker lens we have assumed that it is somewhat blunt and set its length to 0.09 m. This brings the total length of the PGMM to 0.860 m, including the nose and tail tube end, and the aerodynamic length of the body (including nose and boattail, but excluding the tail tube end) is 0.718 m. The total mass is 16.0 kg, the center of mass is located 0.30 m from the nose tip and the moment of inertia[2] around the y-axis (and z-axis) is 0.435 kgm^2.

PGMM geometry for lifting surfaces			
Surface	Chord	Base	Center of pressure
Wing (1 of 4)	0.048	0.140	0.373
Tail fin (1 of 4)	0.025	0.080	0.740
Strake (1 of 4)	0.140	0.025	0.700

Table 2.1: Geometric characteristics of the lifting surfaces. The center of pressure position (assumed constant) for each surface is measured along the body x-axis from the tip of the nose and the total aerodynamic body length is 0.718 m (not counting the tail tube end; with tail tube end the length is 0.860 m).

PGMM mass distribution			
Component	Length [m]	Mass loc. [m]	Mass [kg]
Seeker lens assembly	0.090	0.060	1.5
Navigation electronics	0.058	0.119	1.0
Warhead and fuze	0.180	0.238	8.5
Batt., ctrl. & tail	0.390	0.538	5.0

Table 2.2: The length of each of the five sections of the PGMM (cf. Fig. 2.2), the location of its mass contribution (lumped mass model) measured from the tip of the nose, and the mass of each section. In this description, the mass of sections four (battery, guidance/control electronics) and five (tail with actuators) are lumped together. The center of mass is located 0.30 m from the nose tip and the total mass is 16.0 kg.

We have based the mass distribution on reasonable estimates of the masses for the various parts of the PGMM and not on any detailed calculations. This means in particular that the angle of attack required for constant velocity glide ($1g$-flight) is not exactly the same as the angle of attack which gives optimal lift to drag ratio (cf. Chap. 3) at constant airspeed glide. Hence, there is room for improvement in the matching of aerodynamic and mass distribution properties.

[1] The tail fins are assumed to deploy immediately after the PGMM has left the barrel, to give aerodynamic stability, but the wings deploy at apogee, to minimize drag.

[2] A value for the moment of inertia around the x-axis is not needed in this work.

3 Aerodynamics

The two most important aerodynamic performance indicators are the lift and drag curves. The lift curve determines turn performance and the drag curve determines energy loss during maneuvering as well as coast. Together the two curves also give the aerodynamic efficiency which is the lift to drag ratio, also called the glide number, which delimits the radius of action in non-powered flight. In this chapter we shall describe how these and some related characteristics are modeled for the PGMM using so called handbook methods.

From an aerodynamics modeling perspective, the PGMM is made up from two distinct types of parts; (slender) body and (thin) lifting surfaces. The location and geometry of the lifting surfaces were described in the previous chapter. The body is assumed to consist of three subparts; nose, main body and tail. Together these parts define the aerodynamic characteristics of the missile.

We shall use the method in (Fleeman, 2006) and compute contributions (lift, drag etc.) from the various parts of the missile and simply add them together to form a total contribution. Thus, the aerodynamic model buildup is done without regard to interference effects, such as wing-body interactions[1] or downwash from the wings on the tail fins. This approach is reasonable given the level of fidelity in the modeling we aim for here.

3.1 Flight Envelope and Mission Profile

We consider here a flight envelope[2] of altitudes $h \leq 3000$m, subsonic Mach numbers; airspeed $V \leq 300$m/s at sea level, and an angle of attack[3] $\alpha \leq 20^\circ$.

The generic mission profile consists of launch from sea level at a muzzle velocity of 300m/s or less, where the tail fins deploy immediately after launch. Apogee, which occurs approximately 3000m downrange, is typically at an altitude $h = 2000$m where the wings deploy and glide begins. The airspeed at glide is $V = 125$m/s and with a glide ratio of approx. 4.25 the maximum range is about 11500m. In many cases, however, the seeker opens at about $h = 1000$m (or higher) and the missile dives and maneuvers the last part of the trajectory, which makes the range shorter. The maneuvering is done in order to satisfy terminal constraints in the form of a specified incidence angle on the target or specified direction of approach (in e.g. urban environments), to satisfy constraints for the warhead or to pursuit and hit a moving target such as a ground vehicle.

In the analysis of flight performance we assume that the PGMM is operated in "+" mode, i.e. the flight trajectory is such that the z-axis in the body system B (cf. Section 3.2) is (approximately) aligned with the z-axis in the Earth frame E. The difference between this and "x" mode operation (where the z-axis in B is at a 45° angle with the z-axis in the Earth frame E) is small however, and one can approximately consider the glide and turn performance[4] as independent of the relative angle between the z-axis in B and E.

[1] Many well known handbook methods take also this into account, cf. (Pitts *et al.*, 1957).

[2] We use the ISA atmosphere model (Standard Atmosphere, 1975), (Boiffier, 1998, p. 88).

[3] In this chapter the angle of attack (and local angle of attack for lifting surfaces) is always nonnegative.

[4] A disadvantage with the "+" mode is that it usually is unstable in roll (Fleeman, 2006, p. 72), but since we develop here a performance model (eventually with controller) without regard to roll properties, this is not important.

3.2 Coordinate System

We assume that the body fixed coordinate system B for the missile is Cartesian and has a standard orientation for the axes (x-axis forward, y-axis pointing out over the right wing and z-axis pointing downwards in the vehicle, cf. (Stevens & Lewis, 2003)), as mentioned in the previous chapter. Later we shall exploit symmetries between the dynamics in the xy and xz-planes which exist for many missiles and therefore mostly concentrate on the dynamics in the xz-plane, the pitch plane. It turns out that also for many aspects of the aerodynamics modeling it is sufficient to restrict attention to the xz-plane, but not for all.

The (total) aerodynamic force component f_z along the z-axis in B is essentially only dependent on the angle of attack α and likewise the aerodynamic force component f_y along the y-axis in B is essentially only dependent on the sideslip angle β, for small values of these angles. (For definitions of α, β see (4.9) below.) Therefore, considering only the the xz-plane in B in the aerodynamics modeling would give results for the force component f_z that are transferable to the force component f_y in the xy-plane using symmetry, and vice versa, as long as α, β are small. A similar interchangeability exists, by symmetry, between the aerodynamic pitch and yaw moment. The force component f_x along the x-axis in B is approximately proportional to the total angle of attack α_t, given by $\tan^2(\alpha_t) = \tan^2(\alpha) + \tan^2(\beta)$, and can therefore approximately be obtained by adding contributions due to angle of attack α and sideslip angle β computed separately.

For these reasons, we have chosen to restrict attention in this chapter to the pitch plane in B, and in particular we define lift and drag in terms of the force components f_x and f_z. This means that the results here for f_z are transferable for results for f_y, by using symmetry, and likewise for the pitch and yaw moments. As a consequence, all results in the following chapter which relate to the simplified pitch plane dynamics models are immediately transferable to the yaw plane. For the study of glide ratio in this chapter it is moreover reasonable to stay confined to the pitch plane in B. It is basically only when one considers a maneuvering missile, such as when describing the evolution of airspeed V in the next chapter, that one must consider the pitch and yaw planes simultaneously. In particular, when calculating f_x one must use both α and β (i.e. α_t) in order to correctly determine the induced drag (see below).

3.3 Lift

The normal force coefficient C_N is the aerodynamic coefficient expressing aerodynamic normalized force in the direction of the negative z-axis in B. It is related to the lift coefficient C_L, expressing normalized aerodynamic force in a direction perpendicular to the velocity vector in the xz-plane in B, as

$$C_L = C_X \sin(\alpha) + C_N \cos(\alpha), \tag{3.1}$$

where α is the angle of attack in the xz-plane and C_X is the (positive) axial force coefficient expressing normalized force in the positive x-axis direction in B (Stevens & Lewis, 2003, p. 84). The normal force coefficient C_N for the entire vehicle is obtained as a sum of partial normal force coefficients from the body and the various lifting surfaces, cf. (Fleeman, 2006, p. 78). This represents an instance of the simplified handbook approach described in the beginning of the chapter.

3.3.1 Contributions to lift

The normal force coefficient $C_{N,body}$ for the body of the missile is predicted (using slender body theory and body crossflow theory) by the formula (Fleeman, 2006, p. 36), (cf. (Jorgensen, 1973; Pitts *et al.*, 1957) and (Aiello & Bateman, 1979, p. 39ff))

$$C_{N,body} = \sin(2\alpha)\cos(\alpha/2) + \frac{2\ell}{d}\sin^2(\alpha), \tag{3.2}$$

where $\ell = 0.718$ m is the aerodynamic length of the body (nose, main body and boattail) and $d = 0.12$ m is the diameter. The formula is generally valid for a body fineness $\ell/d > 5$. The center of pressure $x_{cp,body}$ for the body (the point where the moment caused by the aerodynamic normal force vanishes (Pamadi, 2004, Sec. 1.5.2)), measured from the tip of the nose, can be predicted (using slender body theory and crossflow theory) by (Fleeman, 2006, p. 20) (cf. (Pitts *et al.*, 1957), (Jorgensen, 1973))

$$x_{cp,body} = 0.63\ell_{lose}(1 - \sin^2(\alpha)) + 0.5\ell_{body}\sin^2(\alpha),$$

where ℓ_{nose}, ℓ_{body} are the length of the nose and body, respectively (all lengths in the same unit).

For the lifting surfaces (wings, tail fins and strakes) the normal force coefficient $C_{N,surf}$ is predicted (using slender wing theory and Newtonian impact theory) by the formula (Fleeman, 2006, p. 45) (cf. (Tavares, 1990, p. 86))

$$C_{N,surf} = \frac{\pi AR_{surf}}{2}\frac{S_{surf}}{S_{ref}}\big(\sin(\alpha_{loc})\cos(\alpha_{loc}) + 2\sin^2(\alpha_{loc})\big), \tag{3.3}$$

where subscript 'surf' refers to the surface in question, $S_{ref} = \pi(d/2)^2 = 0.011$ m^2 is the reference area of the missile and AR_{surf} is the aspect ratio. In (3.3) the angle of attack variable α_{loc} is the local angle of attack, as it appears over the surface in question for a given flight condition and control surface deflection. The formula is most accurate for low aspect ratios $AR_{surf} < 3$. For a rectangular wing, the aspect ratio AR is given by $AR = b/c$ where b is the base and c is the chord length. The center of pressure (which is the same as aerodynamic center for symmetric airfoils, cf. (Pamadi, 2004, Sec. 1.5.2)) can be predicted (using lifting line theory) to lie at $0.25c$ from the leading edge of the wing for wings with an aspect ratio larger that about 1.5 (Pitts *et al.*, 1957, Chart 11).

Both (3.2) and (3.3) are independent of Mach number, but the latter is more applicable for subsonic and low supersonic Mach numbers. A plot of the normal and lift force coefficients for the body and each of the lifting surfaces is given in Figure 3.1, and in Figure 3.2 the total is given.

The lift force f_L, normal force f_N and axial force f_x are computed from the aerodynamic coefficients C_L, C_N and C_X as (Stevens & Lewis, 2003, p. 76)

$$f_L = \frac{1}{2}\rho V^2 S_{ref} C_L, \quad f_N = \frac{1}{2}\rho V^2 S_{ref} C_N, \quad f_x = \frac{1}{2}\rho V^2 S_{ref} C_X, \tag{3.4}$$

where where ρ is the air density and V is the airspeed, so a linear relation between the three is obtained by a simple scaling both sides of (3.1). An example of the resulting lift force curve is given in Figure 3.3.

3.3.2 Turn performance

3.3.2.1 Normal ("cross wind") acceleration

Normal acceleration in B is defined as a multiple of the (total) force in B which acts perpendicular to the velocity vector (cf. Section 4.4.3 below). In

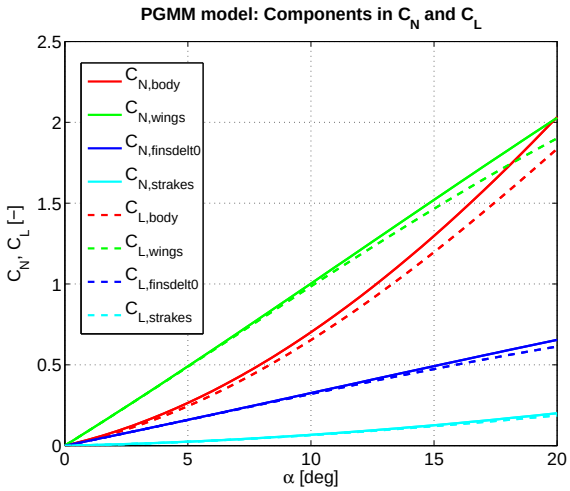

Figure 3.1: Normal and lift coefficient C_N, C_L, respectively, as a function of angle of attack α for the body and a pair of each of the lifting surfaces listed in Table 2.1 for the PGMM, predicted according to the formulas (3.2) and (3.3), respectively. For the lifting surfaces, the value of the angle of attack variable α refers to the local angle of attack (the tail fins are set at zero deflection).

the xz-plane the (normalized) aerodynamic contribution to normal acceleration is defined by the ratio f_L/f_W, where f_W for the PGMM is given by $f_W = mg = 157.0$ N with the mass $m = 16.0$ kg and gravitation acceleration constant $g = 9.81$. An example of the aerodynamic normal acceleration for the PGMM is shown in Figure 3.4. Since the lift curve is essentially linear in α, so is the aerodynamic normal acceleration curve. As an example, to maintain a turn with (normalized) normal acceleration of $2g$ we see that an angle of attack of about 16° is required, if we disregard gravity.

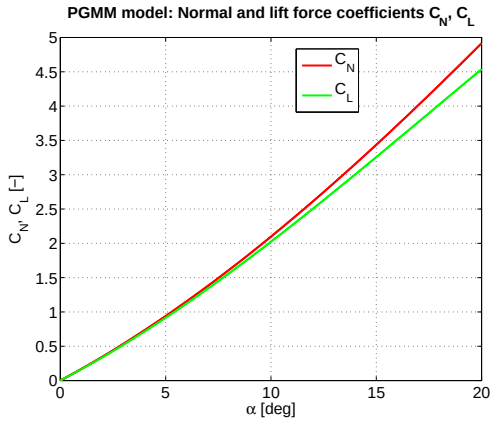

Figure 3.2: Total normal and lift coefficient C_N, C_L, respectively, for the PGMM as defined by the sum of the contributions in Figure 3.1 (tail fins at zero deflection)

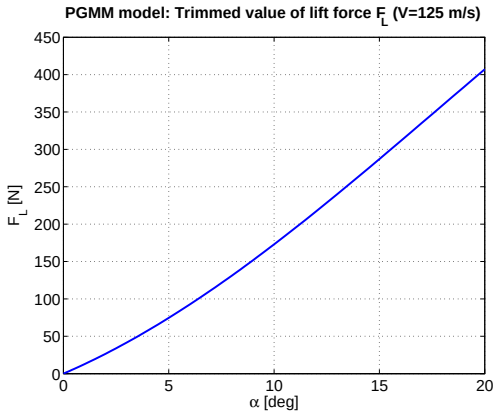

Figure 3.3: Lift force f_L as a function of angle of attack α for the PGMM at the airspeed $V = 125$m/s and altitude $h = 1500$m (tail fins set for zero static pitch moment; "trimmed" position).

3.3.2.2 Turn radius

For circular motion we have the simple relation

$$ar = v^2$$

between magnitude of velocity v, acceleration a and the turning radius r. It follows that the turning radius for the PGMM in a gravity free turn can be

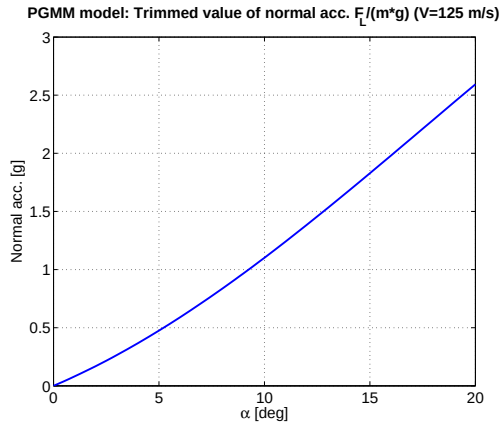

Figure 3.4: Aerodynamic normal acceleration $f_L/(mg)$ as a function of angle of attack α for the PGMM at the airspeed $V = 125$m/s and the altitude $h = 1500$m (tail fins set for zero static pitch moment). The figure shows that an angle of attack of approximately 9° is required to compensate for gravity and obtain force equilibrium in the vertical direction in the Earth fixed frame E (assuming a small flight path angle), for this flight condition. At an angle of attack of approx. 16° an aerodynamic normal acceleration (no gravity) of $2g$ is obtained, which corresponds to a turn radius of close to 800m at $V = 125$m/s. (The turn radius is ideally independent of airspeed, for fixed altitude.)

predicted by (cf. (Fleeman, 2006, Sec. 5.8))

$$r = \frac{V^2}{f_L(\alpha)/m} = \frac{V^2/g}{f_L(\alpha)/(mg)} = \frac{mV^2}{\rho S_{ref} C_L(\alpha) V^2/2} = \frac{2f_W}{g\rho S_{ref} C_L(\alpha)}, \quad (3.5)$$

where we have made the dependence on the angle of attack α explicit. Thus, the turning radius is (ideally) independent of the velocity and the minimal turning radius for a given altitude (i.e. air density ρ) is determined by the maximal allowed angle of attack α. If we limit the angle of attack α to 20° we see from (3.4), (3.5) and Figure 3.3 that at the altitude $h = 1500$m and airspeed $V = 125$m/s the maximal normal acceleration possible to obtain (without gravity) is close to $2.6g$, which gives a minimal turning radius of approximately 615m. At sea level an angle of attack $\alpha = 20°$ gives a normal acceleration of approx. $3g$ for the same airspeed, and the minimal turn radius deceases to about 530m. Limiting the angle of attack to $\alpha \leq 20°$ is reasonable for the PGMM (due to considerations regarding actuators and control system) as will be shown in the next chapter.

3.3.2.3 Turn rate (and normal acceleration revisited)

For circular motion we also have the relation

$$\omega = \frac{v}{r} = \frac{a}{v},$$

between turn rate (angular velocity) ω, and turning radius r and velocity v. Thus, the turn rate can be computed from only knowledge of the velocity and the normal acceleration. As an example, we see that for a $2g$-turn at an airspeed of $V = 125$m/s the turn rate will be approx. 0.157 rad/s (8.99°/s).

Turn rate measures the ability to make changes in the heading angle for the missile but since it is directly proportional to normal acceleration for a given velocity it is often more appropriate to revert back to considering normal acceleration. This is particularly true in end game scenarios using variants of proportional navigation (PN) (Zarchan, 1994) against maneuvering targets. In order for PN to be successful against a maneuvering target the missile will need to have not only a velocity advantage but also an acceleration advantage, the latter often in the order of a factor 3 compared to the target (Zarchan, 1994, Ch. 8).

It is therefore instructive to compute the normal acceleration for maximal angle of attack $\alpha = 20°$ at sea level and for a higher airspeed, which could be the result of a dive and pursuit of a moving target on the ground. An angle of attack $\alpha = 20°$ at sea level and airspeed $V = 170$m/s gives an aerodynamic contribution to normal acceleration of approx. $5.5g$ (and a turn rate of 0.317 rad/s, i.e. 18.2°/s). As a comparison, a normal acceleration of $1g$ for a vehicle moving on the ground at a velocity of 40km/h corresponds to a turning radius of about 12.6 m, which is a rather sharp turn.[5]

3.4 Drag

The drag coefficient C_D expresses the normalized force in the negative direction of the velocity vector in B (Stevens & Lewis, 2003, p. 79). In analogy with (3.4) the drag force f_D is given by

$$f_D = \frac{1}{2}\rho V^2 S_{ref} C_D.$$

[5] Vehicles travelling on ordinary roads rarely exceed lateral acceleration levels of $1g$, which is the limit imposed by the grip of ordinary tires (Blundell & Harty, 2004, p. 6), (Karnopp, 2004, p. 66).

When restricting attention to the xz-plane the drag force coefficient is related to the axial and normal force coefficients, respectively, as

$$C_D = -C_X \cos(\alpha) + C_N \sin(\alpha). \tag{3.6}$$

The drag coefficient for the entire missile is calculated as a sum of contributions of drag coefficients from body and lifting surfaces, just as with the lift coefficient. Normally, the drag coefficient is divided into two principal parts as (Stevens & Lewis, 2003, p. 80)

$$C_D = C_{D0} + C_{Di}, \tag{3.7}$$

where C_{D0} models the so called parasite drag[6] (form drag and friction drag), which is independent of the angle of attack α, and C_{Di} models the induced drag ("drag due to lift"), which is dependent on α. (For a body which is symmetric when mirrored in the xy-plane in B, such as the missile body itself or a symmetric airfoil, the induced drag coefficient C_{Di} is zero when $\alpha = 0$.)

As stated earlier, we shall in this chapter restrict attention to the xz-plane and this means that in order to translate the results here for the induced drag to the general case (not restricted to the xz-plane) one must substitute[7] the angle of attack α for the total angle of attack α_t.

3.4.1 Parasite drag

For a slender missile in subsonic coast the parasite drag for the body is made up of form drag and friction drag, where the form drag is mostly due to base drag effects, i.e. flow separation effects around the tail. A boattail can reduce these effects and therefore it is common to have some form of gradual decrease of the body diameter near the tail, such as the boattail of the PGMM in Figure 2.2. The total parasite drag coefficient $C_{D0,body}$ for the body of the missile is thus

$$C_{D0,body} = C_{D0,bodybase} + C_{D0,bodyfric}, \tag{3.8}$$

where the subscripts indicate base and friction components.

The base drag coefficient for the body of a slender missile with flat base in subsonic (non-powered) coast can be predicted by (Fleeman, 2006, p. 32)

$$C_{D0,bodybase} = 0.12 + 0.13M^2, \tag{3.9}$$

where $M = V/V_a$ is the Mach number defined by the airspeed V and the speed of sound V_a. When the missile has a boattail the coefficient $C_{D0,bodybase}$ is reduced by a certain factor (which essentially translates the base drag to that of a body with smaller base), for the PGMM the factor used is 0.5.

The body friction coefficient for a missile can be predicted by (Fleeman, 2006, p. 32) (cf. Jerger (1960))

$$C_{D0,bodyfric} = 0.053\left(\frac{\ell}{d}\right)\left(\frac{M}{\bar{q}_{psf}\ell_{ft}}\right)^{0.2}, \tag{3.10}$$

where ℓ, d is the missile length and diameter (in the same unit), respectively, ℓ_{ft} is the missile length in feet and $\bar{q}_{psf}$ is the dynamic pressure $\rho V^2/2$ expressed in pounds per square foot.

[6] A third component, the wave drag, is present in C_{D0} at transonic and supersonic Mach numbers, but this is not present here since we only consider a subsonic flight envelope for the PGMM.

[7] This means that the contributions to the induced drag from the lifting surfaces must be adjusted to the situation with flight at a nonzero sideslip angle.

For thin lifting surfaces the form drag part of the parasite drag can be neglected and the parasite drag $C_{D0,surf}$ consists thus (at subsonic speeds) only of the friction drag $C_{D0,surffric}$, i.e.

$$C_{D0,surf} = C_{D0,surffric}. \tag{3.11}$$

The friction drag coefficient $C_{D0,surffric}$ for a thin lifting surface (with two sides wetted) can be predicted by (Fleeman, 2006, p. 49) (cf. Jerger (1960))

$$C_{D0,surffric} = 2\frac{S_{surf}}{S_{ref}} 0.0133 \Big(\frac{M}{\bar{q}_{psf} c_{ft}}\Big)^{0.2}, \tag{3.12}$$

where c_{ft} is the (mean aerodynamic) chord of the lifting surface in units of feet.

3.4.2 Induced drag

The induced drag coefficient $C_{Di,body}$ for the body of a missile can be predicted by the simple formula (Simon & Blake, 1999)

$$C_{Di,body} = C_{L,body} \sin(\alpha),$$

(which is a reasonable approximation considering (3.1) and (3.6)) and the prediction is valid for angles of attack α up to about 30°. For a lifting surface the induced drag coefficient $C_{Di,surf}$ can be predicted (using slender wing theory) with the classic formula (Stevens & Lewis, 2003, p. 80)

$$C_{Di,surf} = \frac{C_{L,surf}^2}{\pi e_f AR_{surf}},$$

where $C_{L,surf}$ is the lift coefficient for the surface in question (computed for the local angle of attack α_{loc}) and e_f is the efficiency factor, which depends on the geometry. For a rectangular wing the efficiently factor is 0.7, and this is the value used for all lifting surfaces of the PGMM.

In Figure 3.5 different contributions to the drag coefficient C_D of the PGMM are shown (the friction coefficients for the tail fins and strakes are omitted since they are very small) and in Figure 3.6 the total drag value of C_D is shown. An example of the resulting drag force curve is given in Figure 3.7.

3.5 Aerodynamic Efficiency

The aerodynamic efficiency of a lifting body or surface is often measured in terms of the lift-to-drag ratio f_L/f_D (Pamadi, 2004, p. 71), (Fleeman, 2006, p. 36). When referred to an entire vehicle it is commonly called the glide ratio. In Figure 3.8 an example of the glide ratio for the PGMM is plotted. The glide ratio can give an estimate of the glide angle, i.e. flight path angle γ for coast with constant airspeed V (Stevens & Lewis, 2003, p. 100) (and this angle is unique, for fixed V, see below). To see this one needs to write down the force balance equations for constant airspeed glide, and this is most often done in the vertical plane "wind axes" (Pamadi, 2004, p. 74) since this gives simpler equations. However, it is useful also to write the balance equations in the vertical and horizontal directions directly since properties of the solutions are more apparent then.

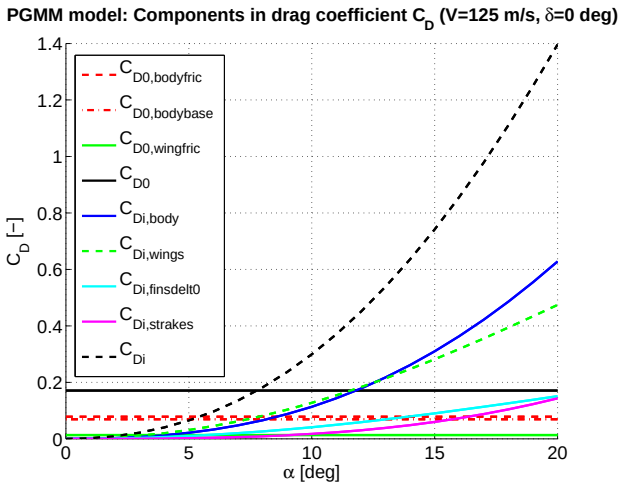

Figure 3.5: Various components of the drag coefficient C_D as a function of the angle of attack α for the PGMM at the airspeed $V = 125$m/s and altitude $h = 1500$m. The angle of attack variable α for the lifting surfaces refers to the local angle of attack over a surface (the tail fin deflection is set to zero).

3.5.1 Glide angle

If the airspeed is held fixed at some value V, the vertical and horizontal balance equations for glide can be written on matrix-vector form as

$$\underbrace{\begin{bmatrix} \cos(-\gamma) & \sin(-\gamma) \\ \sin(-\gamma) & -\cos(-\gamma) \end{bmatrix}}_{\boldsymbol{R}_\gamma} \begin{bmatrix} f_L(\alpha) \\ f_D(\alpha) \end{bmatrix} = \begin{bmatrix} f_W \\ 0 \end{bmatrix}, \tag{3.13}$$

where $\gamma \in [-\pi/2, \pi/2]$ per definition. Under the assumption that there exists an interval $[0, \hat{\alpha}]$ of values of α such that the equation

$$f_L^2(\alpha) + f_D^2(\alpha) = f_W^2 \tag{3.14}$$

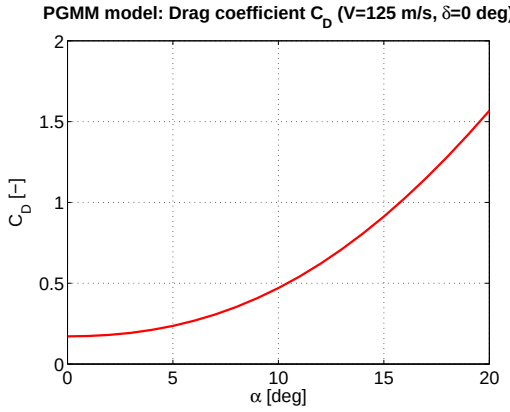

Figure 3.6: Total drag coefficient C_D for the contributions shown in Figure 3.5 (tail fins set to zero deflection).

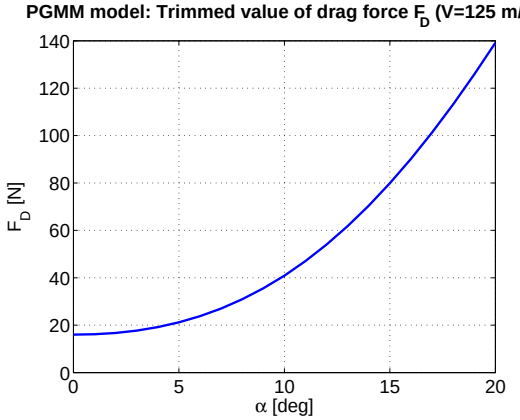

Figure 3.7: Drag force f_D as a function of angle of attack α for the PGMM at the airspeed $V = 125$m/s and altitude $h = 1500$m (tail fins set for zero static pitch moment).

has a unique solution $\alpha \in [0, \hat{\alpha}]$ the system of equations (3.13) has a unique solution $(\alpha, \gamma) \in [0, \hat{\alpha}] \times [-\pi/2, 0]$. Such a value of f_W can be called admissible.[8] The assumption about uniqueness in (3.14) is fulfilled for many aerodynamic configurations, in particular for the PGMM since both f_L, f_D are monotonically increasing functions of α up to stall (which can be used to define $\hat{\alpha}$), cf. Figures 3.3 and 3.7.

To see how the solution to (3.13) can be obtained we note that matrix $\boldsymbol{R}_\gamma$ on the left in (3.13) is symmetric and involutive ($\boldsymbol{R}_\gamma^2 = \boldsymbol{I}$), so it preserves the 2-norm of a vector. The solution is therefore obtained by choosing (the unique admissible) α such that (3.14) is fulfilled (so that the two sides of (3.13) have

[8] Thus, any weight that can be balanced by the *magnitude* of the aerodynamic forces gives a glide solution, i.e. a solution (α, γ) to (3.13).

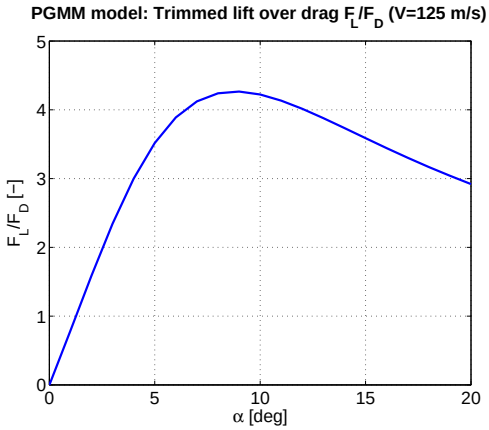

Figure 3.8: Ratio f_L/f_D of lift force over drag force (glide ratio) for the PGMM as a function of angle of attack α for the PGMM at the airspeed $V = 125$m/s and altitude $h = 1500$m (tail fin deflection set for zero pitch moment). The maximum occurs at approx. $\alpha = 9°$ and the value then obtained is approx. 4.25.

equal magnitude) and then γ so that the first row on the left is positive and the second row vanishes (i.e. so that the two sides of (3.13) also have equal direction in $\mathbb{R}^2$). The second row on the left in (3.13) vanishes precisely when

$$\tan(-\gamma) = \frac{1}{f_L(\alpha)/f_D(\alpha)} \tag{3.15}$$

and since the right hand side here is nonnegative we must have $-\gamma \in [0, \pi/2]$, and then the first row is always positive. Thus, (3.14) and (3.15) together form a necessary and sufficient condition for a solution $(\alpha, \gamma) \in [0, \hat{\alpha}] \times [-\pi/2, 0]$ to (3.13), i.e. a glide solution.

The aerodynamic and mass properties are well matched for glide at a given airspeed V if the solution (α, γ) to (3.13) gives a high value on the aerodynamic efficiency $f_L(\alpha)/f_D(\alpha)$ since this gives a small value on the glide angle γ for this speed. To quantify this we introduce the bound $\hat{\gamma}$ for the glide angle γ at a given airspeed V by

$$\tan(-\hat{\gamma}) = \frac{1}{\hat{R}_{ae}}, \tag{3.16}$$

where is $\hat{R}_{ae}$ the maximal value (over α) of the glide ratio $f_L(\alpha)/f_D(\alpha)$ at the given airspeed. From (3.16) we have $-\hat{\gamma} \leq -\gamma$ for any γ which is part of a solution (α, γ) to (3.13). Thus, by comparing the glide angle γ from (3.13) and $\hat{\gamma}$ from (3.16) over airspeeds V we can quantify how well the aerodynamic and mass properties are matched for glide at a given V, and also determine the value of V which gives an optimal value for γ. In the ideal case, the bound $-\hat{\gamma} \leq -\gamma$ becomes tight for an airspeed that is allowed with respect to the constraints of the missile,[9] and this also occurs for the airspeed where $-\hat{\gamma}$ is minimal.

In Figure 3.9 the glide angle γ is shown for the PGMM model along with the bound $\hat{\gamma}$ and in Figure 3.10 the corresponding angle of attack α for glide with γ is shown. It is clear that the bound $\hat{\gamma}$ in this case becomes tight for a reasonable airspeed since it is attained at the airspeed $V = 128$m/s, which is somewhere in the middle of the range of available airspeeds for coast. However, the airspeed at which $\gamma = \hat{\gamma}$ is not exactly the same as the airspeed at which $\hat{\gamma}$ becomes minimal ($V = 130$m/s), so there is some (small) room for improvement in the matching between aerodynamic and mass properties of the PGMM model (and an accompanying, small, increase in range).

3.6 Aerodynamic Stability

3.6.1 Static stability

The question of aerodynamic static stability[10] is of central importance for control of a missile and is directly related to e.g. the sizing of control surfaces.

3.6.1.1 Static margin

A key indicator for static stability is the (normalized) static margin Δ_{sm} defined (for a missile) as

$$\Delta_{sm} = \frac{x_{cp} - x_{cg}}{d}, \tag{3.17}$$

[9] For the PGMM, these can include mission constraints, such as seeker and data processing constraints or constraints on the travel time.

[10] With static stability we here (somewhat loosely) mean moment equilibrium properties for a non rotating airframe.

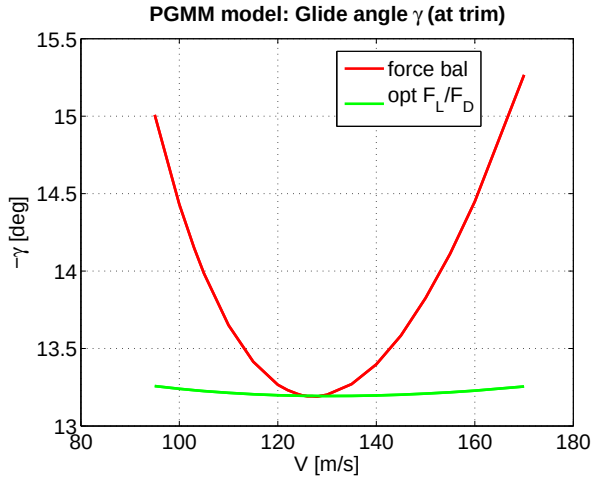

Figure 3.9: Glide angle γ for the PGMM model as a function of airspeed V, at the altitude $h = 1500$m (tail fin deflection set for zero pitch moment). The values shown are obtained by solving the force balance equations (3.13) (upper curve, red) and calculating the bound $\hat{\gamma}$ in (3.16) (lower curve, green). The best value for the glide angle γ is approx. 13.2° obtained at close to $V = 128$m/s and the best value for the bound $\hat{\gamma}$ is slightly less than 13.2° and obtained close to $V = 130$m/s. However, for the entire range $V = 105$–150m/s the glide angle is at most 14°.

where x_{cp}, x_{cg} is the location along the body x-axis, measured from the tip, of the (total) center of pressure and CoM, respectively, and d is the body diameter. In order to have static stability we must have $\Delta_{sm} > 0$. An example of the static margin for the PGMM is shown in Figure 3.11. The static margin is significant for $\alpha = 0$ but approaches neutral stability for $\alpha = 20°$, and the large variation in static margin means that there will be large variation in the short period dynamics (see below).

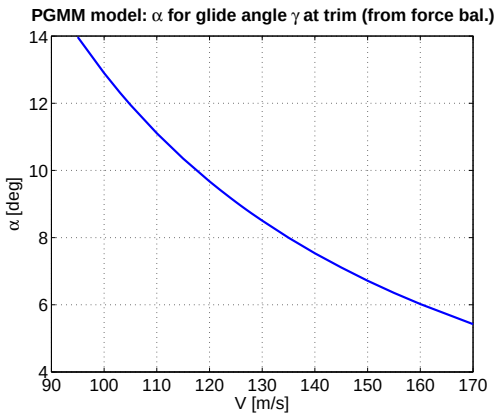

Figure 3.10: Angle of attack α for constant airspeed glide as a function of airspeed V, with the glide angle γ given by the force balance solution in Figure 3.9. For glide at $V = 128$m/s an angle of attack of $\alpha = 8.8°$ is required (approximately).

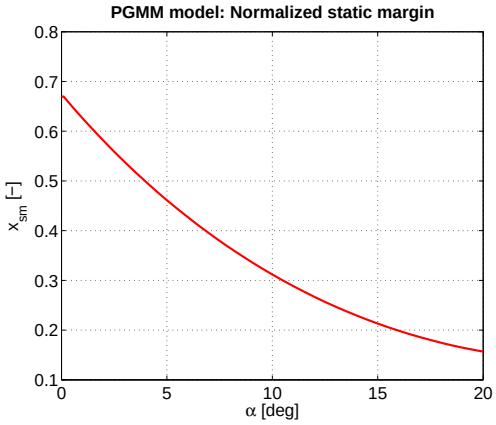

Figure 3.11: Static margin Δ_{sm} as in (3.17) for the PGMM as a function of angle of attack α for the airspeed $V = 125$m/s and altitude $h = 1500$m.

3.6.1.2 Pitch stiffness

The second key indicator for static stability is the pitch stiffness derivative C_{m_α} (Stevens & Lewis, 2003, p. 133) defined as

$$C_{m_\alpha} = \frac{\partial C_m}{\partial \alpha},$$

where C_m is the pitch moment aerodynamic coefficient (Stevens & Lewis, 2003, p. 92ff), (Blakelock, 1991, p. 32ff) describing moment around the positive y-axis in the body system B. For later reference we note that for a non rotating airframe (i.e. zero pitch angular velocity q) the pitch moment coefficient can be approximated by

$$C_m = C_m^{(0)} + C_{m_\alpha}^{(0)} \alpha \tag{3.18}$$

for tail fins at nominal (zero deflection) position and small angles of attack, where $C_{m_\alpha}^{(0)}$ denotes C_{m_α} evaluated at $\alpha = 0$. The term $C_m^{(0)}$ does not depend on α and is zero for a vehicle which is symmetric when mirrored in the xy-plane in B, such as the PGMM. The pitching moment m_y is obtained from C_m as

$$m_y = \frac{1}{2}\rho V^2 S_{ref} c_\ell C_m, \tag{3.19}$$

where ρ, S_{ref} are the air density and reference area, respectively, (cf. Section 3.1, 3.3) and c_ℓ is some characteristic length of the vehicle or significant individual lifting surface (such as the mean aerodynamic chord of a wing). The choice of the reference length c_ℓ is not crucial (since it is only a scaling of C_m, and the latter is really defined in terms of m_y) and here we take

$$c_\ell = d,$$

the diameter of the missile. By symmetry of the missile we assume that the force f_x along the body x-axis does not produce any pitch moment and thus only the force f_z acting along the body z-axis contributes to the pitching moment.

In case not only the static margin but also the overall center of pressure point for the missile is known, such as for the PGMM model where it is obtained

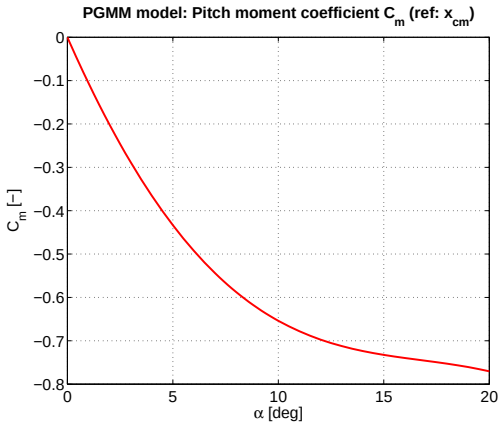

Figure 3.12: Pitch moment (static) coefficient C_m for the PGMM as a function of angle of attack α (tail fins set for zero deflection).

from the aerodynamic component buildup, the value of the pitch moment coefficient C_m can be conveniently computed from C_N using a simple formula. Indeed, we have [11]

$$\frac{1}{2}\rho V^2 S_{ref} d C_m = m_y = -f_N(x_{cp} - x_{cg}) = -\frac{1}{2}\rho V^2 S_{ref} C_N (x_{cp} - x_{cg}).$$

and therefore

$$C_m = -C_N \Delta_{sm}. \tag{3.20}$$

The pitch moment coefficient C_m for the PGMM is shown in Figure 3.12 and the corresponding pitch stiffness derivative C_{m_α} is shown in Figure 3.13. Since the static margin Δ_{sm} is positive for $\alpha \leq 20°$ we know that $C_m \leq 0$ in this region, as can be seen from Figure 3.12. Moreover, $C_{m_\alpha} \leq 0$ for angles of attack $\alpha \leq 20°$, as can be seen from Figure 3.13, which means that if we add

[11] Recall that we have defined x_{cp}, x_{cg} as (positive) distances from the nose tip in accordance with standard missile practice, not as coordinates along the body x-axis.

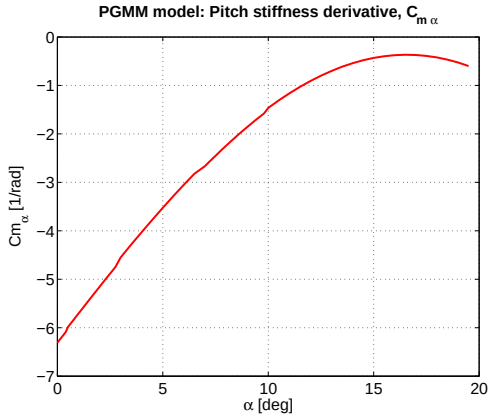

Figure 3.13: Pitch stiffness derivative (static) C_{m_α} for the PGMM as a function of angle of attack α (tail fins set for zero deflection).

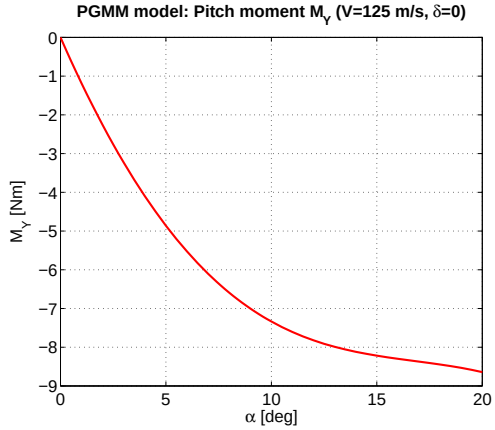

Figure 3.14: Pitch moment (static) m_y for the PGMM as a function of angle of attack α (tail fins at zero deflection) for the airspeed $V = 125$m/s and altitude $h = 1500$m.

a trim moment (via tail fin deflection) to create aerodynamic (static) moment equilibrium for any of these values of α, it will be a (statically) stable point.

In Figure 3.14 an example of the pitching moment for the PGMM is shown (with tail fins at zero deflection). This is the amount of pitch moment that has to be counteracted by tail fin deflection in order to produce zero aerodynamic (static) pitch moment at a given value of the angle of attack.

3.6.2 Static control authority

A requirement for a good matching between aerodynamic design and mass distribution properties is that sufficient control authority exist to produce the necessary trim moments and still have some margin for control (before stall occurs on the control surfaces, due to local angle of attack). As a rough measure of this one can take the ratio (Fleeman, 2006, p. 73)

$$R_{ca} = \left| \frac{\alpha}{\delta_{trim}} \right|,$$

where δ_{trim} is the control surface deflection angle required to produce zero pitch moment for the angle of attack value α. The value of R_{ca} should be larger than 1 for good authority, since most control surfaces have deflection limits in the order of $\pm 30°$ and angles of attack up to $\alpha = 20°$ may need to be trimmed (for zero static pitch moment). This is the case for the PGMM, for example, and the control authority R_{ca} is larger than 1 for the PGMM as can be seen from Figure 3.15. The value for R_{ca} for the PGMM is about 1 for small angles of attack and grows to over 2 for α approaching 15°. The maximal control surface deflection needed for $\alpha \leq 15°$ is just approximately $-6°$ which gives a fair amount of room for motion required by the controller (to synthesize the desired dynamics in pitch), cf. Section 4.5.3.

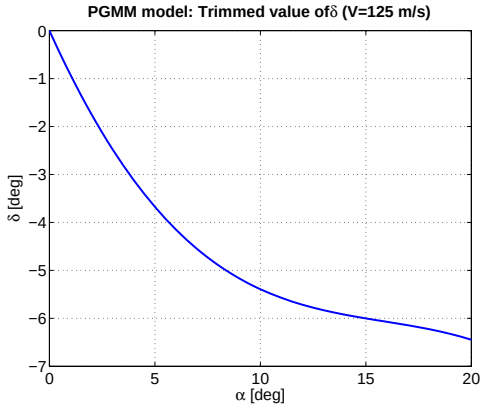

Figure 3.15: Tail fin deflection angle δ (positive for trailing edge down) required for zero (static) aerodynamic pitch moment as a function of angle of attack α for the airspeed $V = 125$m/s and altitude $h = 1500$m. A deflection of approx. $\delta = -5.2°$ is required for pitch moment equilibrium at $\alpha = 9°$.

3.6.3 Dynamic stability

The (open loop) dynamic stability properties[12] of the missile determine how much control authority the control system must have to be able to realize the desired synthesized (closed loop) dynamics.

3.6.3.1 Pitch damping

The key indicator for dynamic stability is the pitch damping derivative C_{m_q} (Stevens & Lewis, 2003, pp. 133-134) defined as[13]

$$C_{m_q} = \frac{\partial C_m}{\partial q},$$

where q is the pitch rate, i.e. the angular velocity around the body y-axis. For a rotating airframe the expression for pitch moment coefficient C_m in (3.18) can be straightforwardly generalized and C_m can thus be approximated by

$$C_m = C_m^{(0)} + C_{m_\alpha}^{(0)}\alpha + C_{m_q}^{(0)}q,$$

for small angles of attack α and pitch rates q, where $C_m^{(0)}$ does not depend on α, q and $C_{m_q}^{(0)}$ denotes C_{m_q} evaluated[14] for $\alpha = q = 0$. There are also instationary effects related to $\dot{\alpha}$ that contribute to C_m, but these are generally smaller and will only be partially taken into account here.

Both the body and tail section contribute to C_{m_q}, and for aircraft the tail contribution is often the largest (Stevens & Lewis, 2003, p. 133). This is true also for slender projectile configurations with tail fins, such as an ordinary mortar round, there the body contribution can be in the order of 15% of the total (Pierens, 1994). For the PGMM however, it turns out that the tail gives the dominant contribution only for small angles of attack.

[12] With dynamic stability we here mean (somewhat loosely) pitch stability properties for a (possibly) rotating airframe.

[13] In the literature there are two forms of this derivative; dimensional and non dimensional (normalized) form. We use here the dimensional form. (For the non dimensional form, as it is defined in aircraft contexts, see e.g. (Stevens & Lewis, 2003, p. 76, 130). In missile contexts the reference length used is often the missile diameter d, cf. (Blakelock, 1991, p. 235ff).)

[14] Strictly speaking we must here also interpret $C_{m_\alpha}^{(0)}$ as being evaluated for $q = 0$.

3.6.3.2 Body

A simple prediction formula for the body related pitch damping effects was derived by A.E. Bryson (1953) based on a variant of slender body theory, and independently also by Sacks (1954). The formula of Bryson and Sacks reads (on dimensional form[15])

$$C_{m_q} + C_{m_{\dot{\alpha}}} = -\frac{d}{u}\left(\frac{\ell - x_{cg}}{d}\right)^2 \frac{\partial C_{N,body}}{\partial \alpha}, \tag{3.21}$$

where $C_{N,body}$ is the contribution to the normal force coefficient C_N from the body, u is the component of the velocity along the body x-axis and, as before, ℓ is the length of the missile, x_{cg} is the distance from the tip to the center of mass and d is the missile diameter. The term $C_{m_{\dot{\alpha}}}$ on the left of (3.21) is the pitch damping derivative due to $\dot{\alpha}$ but this term is usually considerably smaller than[16] C_{m_q} (Weinacht & Danberg, 2005, 2004). Therefore, we shall assume that it can be neglected without sacrificing too much accuracy[17] and we predict C_{m_q} with the formula

$$C_{m_q} = -\frac{(\ell - x_{cg})^2}{Vd} \frac{\partial C_{N,body}}{\partial \alpha}, \tag{3.22}$$

where the partial derivative on the right is evaluated for the value of the angle of attack α which corresponds to trim (static aerodynamic pitch moment equilibrium).

3.6.3.3 Tail

The main mechanism[18] underlying the contribution to C_{m_q} from the tail is the change in angle of attack over the tail fins as the airframe rotates in the airstream and the resulting change in lift contribution from the tail (Stevens & Lewis, 2003, pp. 133-134), (Pamadi, 2004, p. 397), (Blakelock, 1991, p. 237). When we refer to the tail we shall throughout this section mean the combination of tail fins and strakes, since for the PGMM in this context each tail fin and supporting strake can be regarded as one lifting surface.

If we assume that the tail has center of pressure along the body axis of the missile, and aft of the CoM, the contribution $m_{y,tail}$ from the tail to the pitch moment m_y can be written

$$m_{y,tail} = -f_{N,tail}\ell_{tail} = -\frac{1}{2}\rho V^2 S_{ref} \ell_{tail} C_{N,tail}, \tag{3.23}$$

where ℓ_{tail} is the distance from the tail center of pressure to the center of mass and $C_{N,tail}$ is the contribution from the tail to the normal force coefficient.

To derive an expression for the contribution to C_{m_q} from the tail we consider only small angles of attack α and assume, as an approximation, that $C_{N,tail}$ is

[15] Note that Bryson and Sacks use the factor V/d to put the pitch damping coefficient on non-dimensional form, as is often done in missile and projectile contexts.

[16] The figures in (Weinacht & Danberg, 2005, 2004) show the distribution of the contribution to the damping coefficients $C_{m_q}, C_{m_{\dot{\alpha}}}$ over the body length for a slender projectile at various Mach numbers, computed using both computational fluid dynamics calculations and relations of Sacks (including (3.21)) with good agreement between the two.

[17] In fact, as shown in Sect. 4.4.2.1, inserting a value for C_{m_q} which in fact represents the sum $C_{m_q} + C_{m_{\dot{\alpha}}}$ into the simplified short period dynamics relations we shall employ (which do not account for instationary effects) is actually likely to produce a more accurate result.

[18] There is also an effect due to downwash from the wings hitting the tail which gives rise to a term $C_{m_{\dot{\alpha}}}$, but since this effect usually is smaller than C_{m_q} (Stevens & Lewis, 2003, p. 132), (Blakelock, 1991, pp. 236-237) we shall ignore it here.

linear (affine) in the local angle of attack α_{loc}, viz.

$$C_{N,tail} = C^{(0)}_{N,tail} + \frac{\partial C_{N,tail}}{\partial \alpha_{loc}} \alpha_{loc},$$

where $C^{(0)}_{N,tail}$ does not depend on α_{loc} and the derivative should be evaluated for the value of α_{loc} which corresponds to the reference point (angle of attack for body) in question. An instantaneous change in pitch rate Δq produces a corresponding change $\Delta\alpha_{loc}$ in the local angle of attack which depends on both α and α_{loc}. In the simplest case $\alpha = \alpha_{loc} = 0$ the change $\Delta\alpha_{loc}$ is given by

$$\Delta\alpha_{loc} = \arctan\left(\frac{\ell_{tail}\Delta q}{V}\right)$$

and this gives a corresponding change $\Delta C_{N,tail}$ in the value of the normal force coefficient for the tail which is approximately

$$\Delta C_{N,tail} = \frac{\partial C_{N,tail}}{\partial \alpha_{loc}} \Delta\alpha_{loc} = \frac{\partial C_{N,tail}}{\partial \alpha_{loc}} \frac{\ell_{tail}\Delta q}{V},$$

for small values of the ratio $\ell_{tail}\Delta q/V$. From (3.23) it follows that the resulting change Δm_y in pitch moment is

$$\Delta m_y = -\frac{1}{2}\rho V^2 S_{ref}\ell_{tail}\Delta C_{N,tail} = -\frac{1}{2}\rho V S_{ref}\ell^2_{tail}\Delta q \frac{\partial C_{N,tail}}{\partial \alpha_{loc}},$$

so that approximately

$$\frac{\Delta m_y}{\Delta q} = -\frac{1}{2}\rho V S_{ref}\ell^2_{tail}\frac{\partial C_{N,tail}}{\partial \alpha_{loc}}, \tag{3.24}$$

for small values of α, α_{loc} and $\ell_{tail}\Delta q/V$, where the partial derivative on the right is evaluated for $\alpha_{loc} = 0$. This should be compared with the definition of the linear approximation of the effect of a change in q which is

$$\frac{\partial m_y}{\partial q} = \frac{1}{2}\rho V^2 S_{ref} d C_{m_q}. \tag{3.25}$$

Thus, from (3.24) and (3.25) we can conclude that approximately[19]

$$C_{m_q} = -\frac{\ell^2_{tail}}{Vd}\frac{\partial C_{N,tail}}{\partial \alpha_{loc}}.$$

The value of the partial derivative on the right is essentially constant for the tail fins and strakes for a large region of values of α_{loc}, cf. Figure 3.1, and therefore we use the value 1.9 for the fins and the value 0.5 for the strakes (both values estimated from the figure) throughout. The result for body as well as tail, and the total, is shown in Figure 3.16. It can be noted that the large nonlinearity of the body normal force coefficient, cf. Figure 3.1, manifests itself in the contribution from the body to C_{m_q} and that while the tail contribution dominates for angles of attack up to about 2.5°, the body contribution dominates thereafter.

[19] When comparing this to expressions in the literature, in particular ones involving the so called horizontal tail volume ratio (Stevens & Lewis, 2003, p. 134), one should bear in mind that we have used the missile diameter d as reference length in (3.19) and have already included a factor S_{surf}/S_{ref} in the definition of $C_{N,tail}$, cf. (3.3). Moreover, we consider only small values of the angle of attack and we employ the dimensional form on the pitch damping derivative.

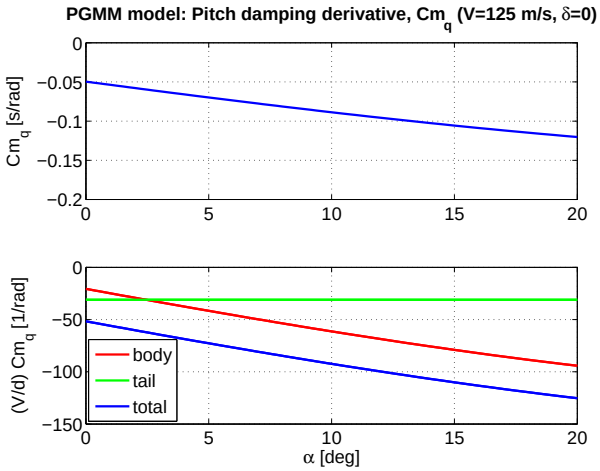

Figure 3.16: Pitch damping derivative C_{m_q} for the PGMM as a function of angle of attack α, for the airspeed $V = 125$m/s. Total value on dimensional form (top) and total as well as components from body and tail on non-dimensional form (bottom).

4 Flight Mechanics

We assume that the missile can be regarded as a rigid body with constant mass distribution, and that the body fixed Cartesian coordinate system B has the origin in the center of mass and that the Earth fixed Cartesian system E is an inertial frame. Moreover, we consider non-powered flight; adding thrust to the model is straightforward.

4.1 Rigid Body Mechanics

The motion of CoM and the motion around CoM can be described by Newton-Euler's equations, which when expressed in B takes the form

$$\begin{aligned} \dot{\boldsymbol{v}} &= \frac{1}{m}\boldsymbol{f} - \boldsymbol{\omega} \times \boldsymbol{v}, && (4.1) \\ \dot{\boldsymbol{\omega}} &= \boldsymbol{J}^{-1}(\boldsymbol{m} - \boldsymbol{\omega} \times \boldsymbol{J}\boldsymbol{\omega}), && (4.2) \end{aligned}$$

where $\boldsymbol{v} = [u, v, w]^T$ is the velocity, $\boldsymbol{\omega} = [p, q, r]^T$ is the angular velocity, $\boldsymbol{f} = [f_x, f_y, f_z]^T$ is the force, $\boldsymbol{m}$ is the moment, m is the mass and $\boldsymbol{J}$ is the moment of inertia matrix which we assume[1] has the form

$$\boldsymbol{J} = \begin{bmatrix} J_{xx} & 0 & J_{xz} \\ 0 & J_{yy} & 0 \\ J_{xz} & 0 & J_{zz} \end{bmatrix}. \tag{4.3}$$

The force vector $\boldsymbol{f}$ is made up of aerodynamic forces and gravity, and therefore we divide the forces f_x, f_y, f_z into aerodynamic components $f_x^{(a)}, f_y^{(a)}, f_z^{(a)}$ and gravity induced components $f_x^{(g)}, f_y^{(g)}, f_z^{(g)}$, respectively, so that[2]

$$\begin{aligned} f_x &= f_x^{(a)} + f_x^{(g)}, \\ f_y &= f_y^{(a)} + f_y^{(g)}, \\ f_z &= f_z^{(a)} + f_z^{(g)}. \end{aligned} \tag{4.4}$$

The moment vector $\boldsymbol{m}$ consists of aerodynamic moments. Aerodynamic missiles are normally controlled using control surfaces forward (canards) or aft (tail fins), and in both these cases deflection of a control surface gives a considerably larger relative change in $\boldsymbol{m}$ than in $\boldsymbol{f}$. It is therefore reasonable, as an approximation, to neglect the force contributions from the control surfaces. Further, it is convenient to partition the moment $\boldsymbol{m}$ as $\boldsymbol{m} = \boldsymbol{m}^{(a)} + \boldsymbol{u}$, where $\boldsymbol{u} = [u_x, u_y, u_z]^T$ is the moment caused by the control surface deflections (from their nominal position) and represents the *control variable*, and $\boldsymbol{m}^{(a)} = [m_x^{(a)}, m_y^{(a)}, m_z^{(a)}]^T$ is the remaining aerodynamic moment (which is mainly due to the orientation of the velocity vector $\boldsymbol{v}$ in B and on $\boldsymbol{\omega}$, for a given Mach number).

[1] If the mass distribution is symmetric when mirrored in the xz-plane we have $J_{xy} = J_{yx} = J_{yz} = J_{zy} = 0$, which is a common assumption common in flight mechanics when the coordinate axes in B have the standard orientation (Stevens & Lewis, 2003). If moreover the mass distribution is symmetric when mirrored in the xy-plane, which can often be assumed for (essentially) cylinder symmetric missiles, we get $J_{xz} = J_{zx} = 0$ and the coordinate axes in B form a principal axes system for the inertia matrix.

[2] Thus, we change notation somewhat compared to the previous chapter where we used the symbols f_x, f_y, f_z to denote aerodynamic components.

To get the complete motion in E it is necessary to complement (4.1), (4.2) with kinematic and dynamic relations which translate the motion to E, e.g.

$$\boldsymbol{V} = \boldsymbol{R}(\boldsymbol{q})\boldsymbol{v}, \tag{4.5}$$

$$\dot{\boldsymbol{q}} = \frac{1}{2}\boldsymbol{q} \circ (0, \boldsymbol{\omega}), \tag{4.6}$$

where $\boldsymbol{V}$ is the velocity for the CoM expressed in E and $\boldsymbol{R}(\boldsymbol{q})$ is the rotation matrix which relates B and E. The rotation matrix $\boldsymbol{R}(\boldsymbol{q})$ is here expressed as a function of an orientation quaternion $\boldsymbol{q}$ (the symbol $\circ$ denotes quaternion multiplication and $(0, \boldsymbol{\omega})$ is the purely imaginary quaternion obtained from the vector $\boldsymbol{\omega}$). In what follows we will focus on different ways to (simplify and) represent the Newton-Euler equations (4.1), (4.2).

Eventually we shall also need Newton's second law of motion for the CoM in E which reads

$$\dot{\boldsymbol{V}} = \frac{1}{m}\boldsymbol{F}, \tag{4.7}$$

where the total force $\boldsymbol{F}$ in E is related to its counterpart $\boldsymbol{f}$ in B as

$$\boldsymbol{F} = \boldsymbol{R}(\boldsymbol{q})\boldsymbol{f}. \tag{4.8}$$

4.2 Partitioning the Dynamics

When working with detailed models of the missile dynamics (full 6-DOF models) the motion of the missile is normally calculated by describing $\boldsymbol{f}$ and $\boldsymbol{m}$ in B, and integrating (4.1), (4.2) together with (4.5), (4.6) to translate the motion to E, as outlined above. However, when working with simplified models of the type we shall consider here there are special circumstances which make another partitioning of the calculations preferable.

4.2.1 Aerodynamic coordinates

In aerodynamic contexts it is common to use other coordinates than the Cartesian primarily defined in B, in particular it is common to employ angle of attack[3] α, sideslip angle β and airspeed (or total velocity) V. To make certain relations simpler below we shall here use the definition of β which is common in missile contexts[4]. We therefore introduce α, β and V as[5]

$$\begin{aligned} \alpha &= \arctan(w/u), \\ \beta &= \arctan(v/u), \\ V &= \sqrt{u^2 + v^2 + w^2}, \end{aligned} \tag{4.9}$$

where $\alpha, \beta \in (-\pi/2, \pi/2)$, which gives us the inverse relations

$$u = \frac{V}{D(\alpha, \beta)}, \tag{4.10}$$

$$v = \frac{V \tan(\beta)}{D(\alpha, \beta)}, \tag{4.11}$$

$$w = \frac{V \tan(\alpha)}{D(\alpha, \beta)}, \tag{4.12}$$

[3] In this chapter, unlike the previous, we shall consider more than one symmetry plane of the missile at the same time and therefore we need at least two aerodynamic angles.

[4] This gives a symmetric form of "semi"-spherical coordinates (in aircraft contexts β is usually defined as $\beta = \arcsin(v/V)$).

[5] Since we shall not consider missiles that fly "backwards" or "sideways" there is no practical restriction in making the domain of definition for α, β as "small" as we do.

where $D(\alpha,\beta)$ is defined as

$$D(\alpha,\beta) = \sqrt{1+\tan(\alpha)^2+\tan(\beta)^2}.$$

With these definitions the force equation (4.1) can be expressed in the form of the following three equations (cf. (Johansson, 1998, p. 14))

$$\begin{aligned}
\dot{\alpha} &= \frac{F_\alpha}{V} - p\cos^2(\alpha)\tan(\beta) - r\sin(\alpha)\cos(\alpha)\tan(\beta) + q, && (4.13)\\
\dot{\beta} &= \frac{F_\beta}{V} + p\cos^2(\beta)\tan(\alpha) + q\sin(\beta)\cos(\beta)\tan(\alpha) - r, && (4.14)\\
\dot{V} &= F_V, && (4.15)
\end{aligned}$$

where

$$\begin{aligned}
F_\alpha &= \frac{D(\alpha,\beta)}{m}\big(f_z\cos^2(\alpha) - f_x\sin(\alpha)\cos(\alpha)\big),\\
F_\beta &= \frac{D(\alpha,\beta)}{m}\big(f_y\cos^2(\beta) - f_x\sin(\beta)\cos(\beta)\big),\\
F_V &= \frac{1}{mD(\alpha,\beta)}(f_x + f_y\tan(\beta) + f_z\tan(\alpha)).
\end{aligned}$$

4.2.2 Geometric interpretation

To gain some insight into the geometric meaning of the equations (4.13)–(4.15) it is worthwhile to write these on matrix-vector form as

$$\begin{bmatrix} \dot{\alpha} \\ \dot{\beta} \\ \dot{V} \end{bmatrix} = DG \begin{bmatrix} f_x \\ f_y \\ f_z \end{bmatrix} + H \begin{bmatrix} p \\ q \\ r \end{bmatrix}, \qquad (4.16)$$

where

$$D = \begin{bmatrix} \frac{D(\alpha,\beta)}{mV} & 0 & 0 \\ 0 & \frac{D(\alpha,\beta)}{mV} & 0 \\ 0 & 0 & \frac{1}{D(\alpha,\beta)} \end{bmatrix}, \quad G = \begin{bmatrix} -\sin(\alpha)\cos(\alpha) & 0 & \cos^2(\alpha) \\ -\sin(\beta)\cos(\beta) & \cos^2(\beta) & 0 \\ 1 & \tan(\beta) & \tan(\alpha) \end{bmatrix},$$

and

$$H = \begin{bmatrix} -\cos^2(\alpha)\tan(\beta) & 1 & -\sin(\alpha)\cos(\alpha)\tan(\beta) \\ \cos^2(\beta)\tan(\alpha) & \sin(\beta)\cos(\beta)\tan(\alpha) & -1 \\ 0 & 0 & 0 \end{bmatrix}.$$

The last row $G_{3,1:3}$ in the matrix G spans the same space as the vector $\boldsymbol{v}$, i.e. $[G_{3,1:3}] = [\boldsymbol{v}]$, and this row is moreover orthogonal to the two first rows $G_{1,1:3}, G_{2,1:3}$ (which, in their turn, are linearly independent) so that $[\{G_{1,1:3}, G_{2,1:3}\}] = [\boldsymbol{v}]^\perp$. This explains how the first term on the right in (4.16) "distributes" $\boldsymbol{f} = [f_x, f_y, f_z]^T$ over $[\boldsymbol{v}]$ and $[\boldsymbol{v}]^\perp$, and in particular we see that

$$\dot{V} = F_V = \frac{1}{mV}\boldsymbol{f}^T\boldsymbol{v} = \frac{1}{m}\frac{\boldsymbol{f}^T\boldsymbol{v}}{\|\boldsymbol{v}\|} = \frac{1}{m}\boldsymbol{e}_{\boldsymbol{v}}^T\boldsymbol{f}, \qquad (4.17)$$

where $\boldsymbol{e}_{\boldsymbol{v}}$ is a unit vector in $\boldsymbol{v}$'s direction. Further, we see that the last row $G_{3,1:3}$ in the matrix G is orthogonal to the first two rows $H_{1,1:3}, H_{2,1:3}$ in the matrix H, so that also $[\{H_{1,1:3}, H_{2,1:3}\}] = [\boldsymbol{v}]^\perp$. Thus, the vector $\boldsymbol{\omega} = [p, q, r]^T$ is "distributed" in a similar way over $[\boldsymbol{v}]^\perp$ by the second term on the right in (4.16).

It is moreover clear that there are symmetries in (4.13)–(4.15) which can be used to obtain simplified dynamical models, at least if one as customary in missile control contexts neglect the effect of gravity so that f_x, f_y, f_z is only determined by aerodynamics (which can be motivated for an agile maneuvering missile).

4.3 Simplified Equations

To obtain simplifications to the system (4.13)–(4.15) and (4.2) we shall start by considering the latter equation and investigate what simplifying assumptions are reasonable to make, in particular with regard to the moment of inertia matrix $\boldsymbol{J}$ in (4.3) and the roll rate p in the moment equation (4.2).

4.3.1 Simplified moment equation

For a slender, essentially cylinder symmetric missile one can assume that $|J_{xz}| < J_{xx}$ ($|J_{xz}|$ is generally much smaller than J_{xx}; for an exactly cylinder symmetric missile J_{xz} is zero) and $J_{yy} = J_{zz}$, where J_{xx} is considerably smaller than J_{yy} (often J_{xx} is in the range $J_{yy}/100$ to $J_{yy}/50$).

The rotation of the missile around the body x-axis is expressed by p and the dynamic equation for p can be extracted form (4.2) as

$$\dot{p} = \frac{J_{zz}(qrJ_{yy} - q(pJ_{xz} + rJ_{zz}))}{J_{xx}J_{zz} - J_{xz}^2} + \frac{J_{xz}(pqJ_{yy} - q(rJ_{xz} + pJ_{xx}))}{J_{xx}J_{zz} - J_{xz}^2} + \frac{J_{zz}}{J_{xx}J_{zz} - J_{xz}^2}(m_x^{(a)} + u_x) - \frac{J_{xz}}{J_{xx}J_{zz} - J_{xz}^2}(m_z^{(a)} + u_z).$$

If we introduce the approximation $J_{xz} = 0$ in this equation together with the assumption $J_{yy} = J_{zz}$ the coupling terms with components from $\boldsymbol{J}$ vanish and we get the following simple dynamics

$$\dot{p} = \frac{1}{J_{xx}}(m_x^{(a)} + u_x). \tag{4.18}$$

These dynamics are very straightforward to stabilize with a state feedback controller, e.g. of the simple PID-type, and for this reason skid-to-turn (STT) operated missiles are often assumed to be roll stabilized ($p = 0$) in studies of missile dynamics. Using the same approximations and assumptions ($J_{xz} = 0, J_{yy} = J_{zz}$) we get for the q, r-dynamics

$$\dot{q} = \frac{pr(J_{yy} - J_{xx})}{J_{yy}} + \frac{1}{J_{yy}}(m_y^{(a)} + u_y), \tag{4.19}$$

$$\dot{r} = \frac{qp(J_{xx} - J_{yy})}{J_{yy}} + \frac{1}{J_{yy}}(m_z^{(a)} + u_z). \tag{4.20}$$

Due to (4.18), and an accompanying reasonable assumption of the existence of a separate controller for the roll channel, it is motivated to make the approximation $p = 0$, whereupon also (4.19), (4.20) simplify to

$$\dot{q} = \frac{1}{J_{yy}}(m_y^{(a)} + u_y), \tag{4.21}$$

$$\dot{r} = \frac{1}{J_{yy}}(m_z^{(a)} + u_z). \tag{4.22}$$

Thus, this simple form for the moment equation is obtained when $J_{xz} = 0, J_{yy} = J_{zz}$ and $p = 0$.

Before we proceed we note that the simplified moment equation derived here should not be interpreted to mean that we can later on fix p at 0 in the overall dynamic equations. It merely means that we model the roll rate p as being so slow that it doesn't affect the rigid body dynamics[6] in B, i.e. the roll rate p need not be taken into account for the rigid body dynamics (over shorter time scales) *when attention is restricted to motion in the the body system* B.

4.3.2 Simplified force equation

If we use the approximation $p = 0$ in (4.13), (4.14) we obtain

$$\dot{\alpha} = \frac{F_\alpha}{V} - r\sin(\alpha)\cos(\alpha)\tan(\beta) + q, \tag{4.23}$$

$$\dot{\beta} = \frac{F_\beta}{V} + q\sin(\beta)\cos(\beta)\tan(\alpha) - r, \tag{4.24}$$

with F_α, F_β given by the same expressions as before, i.e.

$$F_\alpha = \frac{D(\alpha,\beta)}{m}\big(f_z\cos^2(\alpha) - f_x\sin(\alpha)\cos(\alpha)\big), \tag{4.25}$$

$$F_\beta = \frac{D(\alpha,\beta)}{m}\big(f_y\cos^2(\beta) - f_x\sin(\beta)\cos(\beta)\big). \tag{4.26}$$

With the definitions in (4.4) we can also divide F_α, F_β correspondingly as

$$\begin{aligned} F_\alpha &= F_\alpha^{(a)} + F_\alpha^{(g)}, \\ F_\beta &= F_\beta^{(a)} + F_\beta^{(g)}, \end{aligned}$$

where

$$F_\alpha^{(a)} = \frac{D(\alpha,\beta)}{m}\big(f_z^{(a)}\cos^2(\alpha) - f_x^{(a)}\sin(\alpha)\cos(\alpha)\big), \tag{4.27}$$

$$F_\beta^{(a)} = \frac{D(\alpha,\beta)}{m}\big(f_y^{(a)}\cos^2(\beta) - f_x^{(a)}\sin(\beta)\cos(\beta)\big), \tag{4.28}$$

and

$$F_\alpha^{(g)} = \frac{D(\alpha,\beta)}{m}\big(f_z^{(g)}\cos^2(\alpha) - f_x^{(g)}\sin(\alpha)\cos(\alpha)\big), \tag{4.29}$$

$$F_\beta^{(g)} = \frac{D(\alpha,\beta)}{m}\big(f_y^{(g)}\cos^2(\beta) - f_x^{(g)}\sin(\beta)\cos(\beta)\big). \tag{4.30}$$

The expressions (4.27), (4.28) for $F_\alpha^{(a)}, F_\beta^{(a)}$ can be simplified somewhat if we note that (4.13)–(4.15) show that f_x mainly has effect on the dynamics for V. Moreover, for a (significantly) maneuvering missile (in non-powered flight) the magnitude of $|f_x^{(a)}|$ is generally much smaller than $\sqrt{(f_y^{(a)})^2 + (f_z^{(a)})^2}$ and it is then motivated to introduce the approximation $f_x^{(a)} = 0$ in (4.27), (4.28).

4.3.3 Simplified (decoupled) nonlinear model

We have seen that it is reasonable to assume that $J_{xz} = 0, J_{yy} = J_{zz}, p = 0$ and under this assumption the missile dynamics are given by (4.21)–(4.24), with

[6] Referring back to an earlier footnote, we know that insisting that $p = 0$ is a non-holonomic restriction so that the dimension of the base manifold, here rotation angles, can actually be reduced. However, in order to be able to drop one of the coordinates on the base manifold one needs to make a coordinate change first.

F_α, F_β given by (4.25), (4.26). For a (significantly) maneuvering missile it can moreover be reasonable to use the approximation $f_x^{(a)} = 0$, as mentioned at the end of the previous section.

Additional simplifications can be obtained if one notes that the aerodynamic force $f_z^{(a)}$ often mainly[7] depends on α (more than on q and β for fix V, if the arguments u, v, w in $f_z^{(a)}$ are expressed in terms of α, β, V) and in a similar way $f_y^{(a)}$ depends mainly on β (Stevens & Lewis, 2003, p. 76). The moment $m_y^{(a)}$ depends mainly on α and q, and $m_z^{(a)}$ depends mainly on β and r. This makes it possible to assume that the coupling between the α-dynamics and β-dynamics in (4.21)–(4.24) through $f_y^{(a)}, f_z^{(a)}$ is generally weak. If we use this assumption together with the assumption that α, β, q, r are small and replace all geometric nonlinearities in (4.23), (4.24), (4.27), (4.28) with their first order approximations in α, β (around $\alpha, \beta = 0$) we obtain a model of the form

$$\dot{\alpha} = \frac{Z(\alpha)}{V} + q + \frac{F_\alpha^{(g)}}{V}, \tag{4.31}$$

$$\dot{\beta} = \frac{Y(\beta)}{V} - r + \frac{F_\beta^{(g)}}{V}, \tag{4.32}$$

$$\dot{q} = M(\alpha, q) + U^{(y)}, \tag{4.33}$$

$$\dot{r} = N(\beta, r) + U^{(z)}, \tag{4.34}$$

where we have introduced the normalized forces[8] and moments[9] according to

$$Z = \frac{f_z^{(a)}}{m}, \quad Y = \frac{f_y^{(a)}}{m}, \quad M = \frac{m_y^{(a)}}{J_{yy}}, \quad N = \frac{m_z^{(a)}}{J_{yy}},$$
$$U^{(y)} = \frac{u_y}{J_{yy}}, \quad U^{(z)} = \frac{u_z}{J_{yy}}. \tag{4.35}$$

In (4.31)–(4.34) there is no coupling between the pitch dynamics in (α, q) and yaw dynamics in (β, r), and the two subsystems are moreover of the same form, after a simple change of variable in the latter (e.g. by $(z, r) \to -(z, r)$ in (4.32), (4.34)). *For this reason we will henceforth consider only the pitch plane part* (4.31), (4.33) *of the simplified rigid body dynamics* (4.31)–(4.34).

For later reference we note that the assumption that α, β, q, r are small makes the expressions for the aerodynamic forces $F_\alpha^{(a)}, F_\beta^{(a)}$ in B simple while the gravity induced components $F_\alpha^{(g)}, F_\beta^{(g)}$ in B become complicated (compared to their counterparts in E). In the Earth fixed frame E the opposite holds, and this observation can be useful in implementations.

---

[7] The q-dependence in $f_z^{(a)}$ is mainly due to the fact a rotation around the y-axis makes the tail fins move relative to the surrounding air which produces a force. This force is however weak for the missiles with small tail fins and we will therefore neglect it here. In a similar way a rotation around the y-axis also produces a moment around this axis, as described in Sect. 3.6.3.1, and also this moment is generally small but we shall still take it into account in $m_y^{(a)}$. Analogous dependencies exist in $f_y^{(a)}$ and $m_z^{(a)}$.

[8] Note that Y, Z, M and N all have implicit dependence on V, cf. (3.4).

[9] To see how the normalized pitch moment in (4.33) can be separated into two parts M and $U^{(y)}$, where $U^{(y)}$ is a control variable (and can be assigned "arbitrary" values), let the (total) normalized pitch moment be $M(\alpha, q, \delta)$ where δ is the control fin deflection. Locally around a reference value δ_r we can write $M(\alpha, q, \delta) = M(\alpha, q, \delta_r) + \tilde{M}(\alpha, q, \delta_r, \delta)(\delta - \delta_r)$, where $\tilde{M}(\alpha, q, \delta_r, \delta)$ has a finite limit as $\delta \to \delta_r$, for any α, q. For any region $\mathcal{D}$ of values α, q and interval $\mathcal{I}$ of values δ such that $\mathcal{I} \ni \delta \mapsto \tilde{M}(\alpha, q, \delta_r, \delta)(\delta - \delta_r)$ is monotone, for fixed $(\alpha, q) \in \mathcal{D}$, we can define the normalized control moment as $U^{(y)} = \tilde{M}(\alpha, q, \delta_r, \delta)(\delta - \delta_r)$. Physically, $\tilde{M}(\alpha, q, \delta_r, \delta)(\delta - \delta_r)$ is the "differential" moment contribution by the control surfaces. Analogous remarks apply for the yaw plane.

4.3.4 Linearized model of the pitch plane dynamics

In order to arrive at (4.31)–(4.34) we linearized the geometric nonlinearities (i.e. used small angle assumptions) and used some assumptions on the aerodynamics. Of course, the decoupling of the pitch and yaw dynamics which is obtained in (4.31)–(4.34) is also obtained by direct (full) linearization around $\alpha, \beta = 0$ of the equations (4.21)–(4.26) if the assumptions $J_{xz} = 0, J_{yy} = J_{zz}, p = 0, f_x^{(a)} = 0$ are used together with the assumptions that $f_z^{(a)}$ depends only on α and that $f_y^{(a)}$ depends only on β (since the middle term on the right in (4.23) and (4.24) vanishes in the linearization.) Alternatively, the equations (4.31)–(4.34) can be linearized with the same result (if $F_\alpha^{(g)}, F_\beta^{(g)}$ are set to zero).

For later use we need to write down how the simplified rigid body equations in the form they appear after linearization around some point α_0, q_0 and for the reasons given at the end of the preceding section we shall here restrict ourselves to consider only the pitch plane dynamics (4.31), (4.33). The linearization is assumed to be performed around a point $\alpha = \alpha_0, q = q_0$ where α_0, q_0 are small (so that (4.31), (4.33) provide a good approximation of the dynamics in the pitch plane) and slowly varying[10] (so that $\dot{\alpha}_0 = 0, \dot{q}_0 = 0$). If we introduce the deviations

$$\tilde{\alpha} = \alpha - \alpha_0, \quad \tilde{q} = q - q_0, \quad \tilde{U} = U^{(y)} - U_0^{(y)}, \tag{4.36}$$

then linearization around α_0, q_0 of the right hand sides in (4.31), (4.33) gives

$$\dot{\tilde{\alpha}} = \frac{Z_\alpha(\alpha_0)}{V}\tilde{\alpha} + \tilde{q} + R_\alpha(\alpha_0, q_0), \tag{4.37}$$

$$\dot{\tilde{q}} = M_\alpha(\alpha_0, q_0)\tilde{\alpha} + M_q(\alpha_0, q_0)\tilde{q} + \tilde{U} + R_q(\alpha_0, q_0), \tag{4.38}$$

where

$$Z_\alpha = \frac{dZ}{d\alpha}, \quad M_\alpha = \frac{\partial M}{\partial \alpha}, \quad M_q = \frac{\partial M}{\partial q}, \tag{4.39}$$

and

$$R_\alpha(\alpha_0, q_0) = \frac{Z(\alpha_0)}{V} + q_0 + \frac{F_\alpha^{(g)}}{V}, \quad R_q(\alpha_0, q_0) = M(\alpha_0, q_0) + U_0^{(y)}. \tag{4.40}$$

It is tempting here to try to chose the reference point (α_0, q_0) so that the remainder terms $R_\alpha(\alpha_0, q_0), R_q(\alpha_0, q_0)$ in (4.40) become zero, but as we shall see this is not always the best choice. We also point out that the gravity induced term $F_\alpha^{(g)}$ depends on the orientation in E of the missile, a fact which must be kept in mind in the following.

4.3.4.1 The case where (α_0, q_0) is an equilibrium point

The reference point (α_0, q_0) is an equilibrium point to (4.31), (4.33) for $\tilde{U} = 0$ if and only if the two remainder terms $R_\alpha(\alpha_0, q_0), R_q(\alpha_0, q_0)$ in (4.40) vanish. For a given α_0, the two remainder terms in (4.40) vanish precisely when $q_0 = q_0^{(g)}$ and $U_0^{(y)} = U_0^{(y,g)}$ where

$$q_0^{(g)} = -\frac{Z(\alpha_0)}{V} - \frac{F_\alpha^{(g)}}{V}, \tag{4.41}$$

[10] If α_0, q_0 cannot be assumed to be slowly varying then $\dot{\alpha}_0, \dot{q}_0$ must be part of $R_\alpha(\alpha_0, q_0)$ and $R_q(\alpha_0, q_0)$, respectively, and the substitutions $F_\alpha^{(g)} \to F_\alpha^{(g)} + \dot{\alpha}_0$ and $U_0^{(y)} \to U_0^{(y)} + \dot{q}_0$ must be made in all of what follows.

and

$$U_0^{(y,g)} = -M(\alpha_0, q_0^{(g)}). \tag{4.42}$$

This choice of reference point is often not the best for a maneuvering missile, as we shall see next.

4.3.4.2 The effect of gravity: I

From (4.41) and (4.42) we see that if we linearize around an equilibrium point $(\alpha_0, q_0^{(g)})$ for (4.31), (4.33) then $q_0^{(g)}$ and $U_0^{(y,g)}$ will always depend on the gravity force term $F_\alpha^{(g)}/V$ and we cannot immediately "extract" the effect of gravity. (In particular, the reference value $q_0^{(g)}$ of the pitch rate which corresponds to a fixed α_0 will then depend on the orientation in E of the missile.) If, however, we chose to linearize around a reference point (α_0, q_0) which is not an equilibrium point for (4.31), (4.33), in particular a reference point which gives equilibrium in the absence of gravity ("aerodynamic equilibrium"), then such an extraction is straightforward (and the reference values will not depend on the orientation of the missile).

For a missile in (essentially) "nominal" position, i.e. with its coordinate axes in B (essentially) aligned with those in E (so that in particular, both z-axes "point downwards") the second term on the right in (4.41) has sign given by $F_\alpha^{(g)}/V > 0$. Thus, if the missile is symmetric with respect to mirroring in the xy-plane in B and $\alpha_0 \geq 0$ then the first term on the right in (4.41) has sign given by $Z(\alpha_0)/V \leq 0$ and it is possible to have $q_0^{(g)} = 0$ for $\alpha_0 \geq 0$, which is necessary for glide flight. If, however, we linearize around a reference point where we disregard gravity the reference value q_0 will not be zero unless α_0 is zero (at least for a missile which is symmetric with respect to the xy-plane).

4.3.4.3 The case where (α_0, q_0) gives aerodynamic equilibrium

A convenient choice for linearization point is to select α_0 and then set $q_0 = q_0^{(a)}$ with $q_0^{(a)}$ given by

$$q_0^{(a)} = -\frac{Z(\alpha_0)}{V}, \tag{4.43}$$

which is the value of q_0 which would have given equilibrium in (4.31) if the missile were flying in a gravity free sea of air, i.e. the value of q_0 which would yield aerodynamic force equilibrium. In this case we get $R_\alpha(\alpha_0, q_0^{(a)}) = F_\alpha^{(g)}/V$. We can still chose $U_0^{(y)}$ so that $R_q(\alpha_0, q_0) = 0$, i.e. we can chose $U_0^{(y)} = U_0^{(y,a)}$ where

$$U_0^{(y,a)} = -M(\alpha_0, q_0^{(a)}), \tag{4.44}$$

which is the value for the normalized tail fin trim moment $U_0^{(y)}$ which gives total moment 0 in (4.33) for $(\alpha_0, q_0^{(a)})$, i.e. aerodynamic moment equilibrium. We are going to refer to a reference point $(\alpha_0, q_0^{(a)})$ of this type as *aerodynamic equilibrium*.

It natural to regard α_0 as an independent parameter and q_0 as a dependent parameter[11] and with $\alpha_0, q_0 = q_0^{(a)}(\alpha_0), U_0^{(y)} = U_0^{(y,a)}$ given by (4.43), (4.44)

[11] Since (4.43) represents a one-to-one correspondence between α_0 and q_0 for a large region of values of α_0 (up to stall) we could equally well have started with q_0 as an independent parameter and then let α_0 be a dependent parameter.

the system (4.37), (4.38) assumes the form

$$\begin{aligned} \dot{\tilde{\alpha}} &= \frac{Z_\alpha(\alpha_0)}{V}\tilde{\alpha} + \tilde{q} + \frac{F_\alpha^{(g)}}{V}, && (4.45)\\ \dot{\tilde{q}} &= M_\alpha(\alpha_0, q_0^{(a)}(\alpha_0))\tilde{\alpha} + M_q(\alpha_0, q_0^{(a)}(\alpha_0))\tilde{q} + \tilde{U}. && (4.46) \end{aligned}$$

Here, gravity becomes an explicit "disturbance" in the force equation (4.45). If the system (4.45), (4.46) is written on matrix-vector form as

$$\begin{bmatrix} \dot{\tilde{\alpha}} \\ \dot{\tilde{q}} \end{bmatrix} = \begin{bmatrix} Z_\alpha(\alpha_0)/V & 1 \\ M_\alpha(\alpha_0, q_0^{(a)}(\alpha_0)) & M_q(\alpha_0, q_0^{(a)}(\alpha_0)) \end{bmatrix} \begin{bmatrix} \tilde{\alpha} \\ \tilde{q} \end{bmatrix} + \begin{bmatrix} F_\alpha^{(g)}/V \\ \tilde{U} \end{bmatrix} \tag{4.47}$$

it is clear that the gravity term $F_\alpha^{(g)}/V$ can simply be regarded as part of the driving signal to the system.

The gravity term in (4.47) can be transformed (by "backstepping"[12]) to an equivalent term acting alongside with $\tilde{U}$ by introducing the new state variable ξ as

$$\xi = \tilde{q} + F_\alpha^{(g)}/V,$$

which gives the equivalent system

$$\begin{bmatrix} \dot{\tilde{\alpha}} \\ \dot{\xi} \end{bmatrix} = \begin{bmatrix} Z_\alpha(\alpha_0)/V & 1 \\ M_\alpha(\alpha_0, q_0^{(a)}(\alpha_0)) & M_q(\alpha_0, q_0^{(a)}(\alpha_0)) \end{bmatrix} \begin{bmatrix} \tilde{\alpha} \\ \xi \end{bmatrix} + \begin{bmatrix} 0 \\ 1 \end{bmatrix} u, \tag{4.48}$$

where

$$u = \tilde{U} + U^{(g)}(\alpha_0)$$

and

$$U^{(g)}(\alpha_0) = -M_q(\alpha_0)\frac{F_\alpha^{(g)}}{V} + \frac{d}{dt}\frac{F_\alpha^{(g)}}{V}.$$

The two systems (4.47) and (4.48) has the same system poles but different transfer functions from input to $\tilde{\alpha}$ since the definition of input signals differ (in particular, one is two-dimensional and the other is one-dimensional).

4.4 Pitch Plane Dynamics

From now on we shall mostly consider the case where the reference point q_0 is given by $q_0^{(a)}$ in (4.43) and it will be convenient to introduce the short form notation

$$\begin{aligned} M_\alpha(\alpha_0) &= M_\alpha(\alpha_0, q_0^{(a)}(\alpha_0)),\\ M_q(\alpha_0) &= M_q(\alpha_0, q_0^{(a)}(\alpha_0)), \end{aligned} \tag{4.49}$$

where the right hand sides are given by (4.39). These short forms are moreover motivated by the fact that the pitch stiffness and pitch damping derivatives $C_{m_\alpha}^{(0)}$ and C_{m_q}, respectively, are often modeled without dependence on the pitch rate q. In the model of the PGMM aerodynamics developed in Chapter 3, for instance, this is the case.

[12]The name backstepping is very natural given how the mathematical operation can be illustrated in block diagram form, see (Khalil, 2002, p. 591).

4.4.1 The short period approximation

The equations for the linearized pitch plane dynamics (4.45), (4.46) around an aerodynamic equilibrium point $(\alpha_0, q_0^{(a)})$ can be written on scalar (SISO) form in terms of the variable $\tilde{\alpha}$ by eliminating $\tilde{q}$ as

$$\begin{aligned}
\ddot{\tilde{\alpha}} &= \frac{Z_\alpha(\alpha_0)}{V}\dot{\tilde{\alpha}} - \frac{Z_\alpha(\alpha_0)\dot{V}}{V^2}\tilde{\alpha} + M_\alpha(\alpha_0)\tilde{\alpha} + M_q(\alpha_0)\tilde{q} + \tilde{U} + \frac{d}{dt}\frac{F_\alpha^{(g)}}{V} \\
&= \frac{Z_\alpha(\alpha_0)}{V}\dot{\tilde{\alpha}} - \frac{Z_\alpha(\alpha_0)\dot{V}}{V^2}\tilde{\alpha} + M_\alpha(\alpha_0)\tilde{\alpha} + M_q(\alpha_0)(\dot{\tilde{\alpha}} - \frac{Z_\alpha(\alpha_0)}{V}\tilde{\alpha} - \frac{F_\alpha^{(g)}}{V}) \\
&\quad + \tilde{U} + \frac{d}{dt}\frac{F_\alpha^{(g)}}{V} \\
&= \big(\frac{Z_\alpha(\alpha_0)}{V} + M_q(\alpha_0)\big)\dot{\tilde{\alpha}} + \big(M_\alpha(\alpha_0) - M_q(\alpha_0)\frac{Z_\alpha(\alpha_0)}{V} - \frac{Z_\alpha(\alpha_0)\dot{V}}{V^2}\big)\tilde{\alpha} \\
&\quad + \tilde{U} - M_q(\alpha_0)\frac{F_\alpha^{(g)}}{V} + \frac{d}{dt}\frac{F_\alpha^{(g)}}{V}. \qquad (4.50)
\end{aligned}$$

The second order linear dynamics described by the differential equation (4.50) is often referred to (for $\dot{V} = 0$) as the *short period approximation* (Ananthkrishnan & Unnikrishnan, 2001) of the pitch plane dynamics.

Using the approximation $\dot{V} = 0$ the short period approximation (4.50) can be parameterized as

$$\ddot{\tilde{\alpha}} + 2\zeta_{sp}(\alpha_0)\omega_{sp}(\alpha_0)\dot{\tilde{\alpha}} + \omega_{sp}^2(\alpha_0)\tilde{\alpha} = \tilde{U} + U^{(g)}(\alpha_0), \qquad (4.51)$$

where

$$\tilde{U} = U^{(y)} - U_0^{(y,a)}, \quad U^{(g)}(\alpha_0) = -M_q(\alpha_0)\frac{F_\alpha^{(g)}}{V} + \frac{\dot{F}_\alpha^{(g)}}{V}, \qquad (4.52)$$

and the natural angular frequency $\omega_{sp}(\alpha_0)$ and damping $\zeta_{sp}(\alpha_0)$, respectively, are given by

$$\begin{aligned}
\omega_{sp}^2(\alpha_0) &= -(M_\alpha(\alpha_0) - M_q(\alpha_0)(Z_\alpha(\alpha_0)/V)), \qquad (4.53) \\
2\zeta_{sp}(\alpha_0)\omega_{sp}(\alpha_0) &= -(M_q(\alpha_0) + Z_\alpha(\alpha_0)/V). \qquad (4.54)
\end{aligned}$$

The expressions (4.53), (4.54) for the natural frequency and damping are the ones often given in the literature to describe the short period approximation[13] (cf. e.g. Ananthkrishnan & Unnikrishnan (2001, Eq. (10)), or Stevens & Lewis (2003, Eq. (4.2-10)) with $Z_{\dot{\alpha}}, Z_q, M_{\dot{\alpha}} = 0$).

The quantities on the right in (4.53), (4.54) can conveniently be expressed in terms of aerodynamic coefficients, for instance we have (cf. Chapter 3)

$$Z_\alpha(\alpha_0) = \frac{1}{m}\frac{\partial f_z}{\partial \alpha}|_{\alpha=\alpha_0} = \frac{1}{2m}\rho V^2 S_{ref}\frac{\partial C_Z}{\partial \alpha}|_{\alpha=\alpha_0},$$

where ρ is the air density, S_{ref} is the reference area and C_Z is the aerodynamic force coefficient in the (positive) z-direction. The other constants can analogously be described in terms of derivatives of the appropriate aerodynamic force and moment coefficients (see Chapter 3).

[13] Usually, however, the linearization point (α_0, q_0) chosen in the literature is the one in (4.41), (4.42) which gives equilibrium for (4.37), (4.38), and the flight condition is straight and level horizontal flight (Ananthkrishnan & Unnikrishnan, 2001).

4.4.1.1 State space representation

For later reference it will be useful with a state space representation of the scalar relation (4.51). The simplest choice of state variables x_1, x_2 is

$$x_1 = \tilde{\alpha}, \quad x_2 = \dot{x}_1$$

which gives the representation

$$\begin{aligned}\begin{bmatrix} \dot{x}_1 \\ \dot{x}_2 \end{bmatrix} &= \begin{bmatrix} 0 & 1 \\ M_\alpha(\alpha_0) - M_q(\alpha_0)\frac{Z_\alpha(\alpha_0)}{V} & \frac{Z_\alpha(\alpha_0)}{V} + M_q(\alpha_0) \end{bmatrix} \begin{bmatrix} x_1 \\ x_2 \end{bmatrix} + \begin{bmatrix} 0 \\ 1 \end{bmatrix} u \\ &= \begin{bmatrix} 0 & 1 \\ -\omega_{sp}^2(\alpha_0) & -2\zeta_{sp}(\alpha_0)\omega_{sp}^2(\alpha_0) \end{bmatrix} \begin{bmatrix} x_1 \\ x_2 \end{bmatrix} + \begin{bmatrix} 0 \\ 1 \end{bmatrix} u, \end{aligned} \tag{4.55}$$

where

$$u = \tilde{U} - M_q(\alpha_0)\frac{F_\alpha^{(g)}}{V} + \frac{\dot{F}_\alpha^{(g)}}{V} = \tilde{U} + U^{(g)}(\alpha_0) \tag{4.56}$$

and $\tilde{U}, U^{(g)}(\alpha_0)$ are defined as in (4.52) (recall that $\dot{V} = 0$ in (4.51)).

4.4.1.2 The effect of gravity: II

It is easy to incorporate "gravity compensation" in (4.55) and (4.56) by simply defining a new reference value $\hat{U}_0^{(y)}$ for the normalized control surface moment $U^{(y)}$ as

$$\hat{U}_0^{(y)} = U_0^{(y,a)} - U^{(g)}(\alpha_0), \tag{4.57}$$

since with this reference value the deviation $U^{(y)} - \hat{U}_0^{(y)}$ becomes

$$U^{(y)} - \hat{U}_0^{(y)} = U^{(y)} - U_0^{(y,a)} + U^{(g)}(\alpha_0) = \tilde{U} + U^{(g)}(\alpha_0),$$

and $(\tilde{\alpha}, \dot{\tilde{\alpha}}) = (0, 0)$ will be an equilibrium point for (4.55) when $U^{(y)} = \hat{U}_0^{(y)}$. Moreover, when $\dot{F}_\alpha^{(g)} = 0$ the reference moment $\hat{U}_0^{(y)}$ is, to first order, equal to the normalized moment $U_0^{(y,g)}$ in (4.42) which yields equilibrium[14] in (4.37), (4.38) for $(\alpha_0, q_0^{(g)})$. To see this, we use the result (4.42), the definitions (4.41), (4.43) for $q_0^{(g)}$ and $q_0^{(a)}$, respectively, and the following linear approximation

$$\begin{aligned} U_0^{(y,g)} &= -M(\alpha_0, q_0^{(g)}) \\ &= -M(\alpha_0, q_0^{(a)}) - M_q(\alpha_0, q_0^{(a)})(q_0^{(g)} - q_0^{(a)}) \\ &= U_0^{(y,a)} + M_q(\alpha_0)\frac{F_\alpha^{(g)}}{V} \\ &= U_0^{(y,a)} - U^{(g)}(\alpha_0), \end{aligned} \tag{4.58}$$

where we also have used the definition of $U^{(g)}(\alpha_0)$ in (4.52) (with $\dot{F}_\alpha^{(g)} = 0$) and the second short form in (4.49). Hence, the reference moment in (4.57) can, under these assumptions, be approximated as

$$\hat{U}_0^{(y)} = U_0^{(y,g)}. \tag{4.59}$$

[14]The very definition of a time invariant equilibrium as in (4.41) requires, for fixed α_0, that the time derivative $(d/dt)(F_\alpha^{(g)}/V)$ vanishes and since we have assumed $\dot{V} = 0$ the condition on the time derivative collapses to $\dot{F}_\alpha^{(g)} = 0$.

4.4.2 Control authority and trimming

We know from the previous section that the control surface induced normalized moment $U^{(y)}$ required to maintain a constant angle of attack α_0 is (for $\dot{V}=0$) given by

$$U^{(y)} = \hat{U}_0^{(y)}$$

where $\hat{U}_0^{(y)}$ is defined in (4.57). To see how large the moment $\hat{U}_0^{(y)}$ can be we invoke the assumption that the normalized pitch damping moment M_q defined in (4.39) is independent of the pitch rate q (i.e. constant as a function of q), as suggested in the beginning of Section 4.4, so that $M_q(\alpha_0, q_0^{(a)}) = M_q(\alpha_0, 0)$. We can then make the following linear approximation

$$\begin{aligned} M(\alpha_0, q_0^{(a)}) &= M(\alpha_0,0) + M_q(\alpha_0,0)q_0^{(a)} \\ &= M(\alpha_0,0) + M_q(\alpha_0)q_0^{(a)} \\ &= M(\alpha_0,0) - M_q(\alpha_0)\frac{Z(\alpha_0)}{V}, \end{aligned}$$

where we have used the definition (4.43) and $M_q(\alpha_0)$ is the short form introduced in (4.49) (applied to the special case where M_q is independent of q). With this approximation we have, using also the definitions (4.41), (4.52) and (4.57), that

$$\begin{aligned} \hat{U}_0^{(y)} &= U_0^{(y,a)} - U^{(g)}(\alpha_0) \\ &= -M(\alpha_0, q_0^{(a)}) + M_q(\alpha_0)\frac{F_\alpha^{(g)}}{V} - \frac{\dot{F}_\alpha^{(g)}}{V} \\ &= -M(\alpha_0,0) + M_q(\alpha_0)\big(\frac{Z(\alpha_0)}{V} + \frac{F_\alpha^{(g)}}{V}\big) - \frac{\dot{F}_\alpha^{(g)}}{V} \\ &= -M(\alpha_0,0) - M_q(\alpha_0)q_0^{(g)} - \frac{\dot{F}_\alpha^{(g)}}{V}. \end{aligned} \tag{4.60}$$

The first term on the right is due to the normalized static aerodynamic pitch moment $M(\alpha_0, 0)$ induced by the airframe (an example of which is given for the PGMM (in unnormalized form) in Figure 3.14). For glide flight the right hand side in (4.60) consists of only this term since then $q_0^{(g)} = 0$ and $\dot{F}_\alpha^{(g)} = 0$ so the last two terms vanish, and the trimming moment required for glide will thus be given by $-M(\alpha_0, 0)$. This also means that for the value of α_0 which corresponds to glide flight the term $M_q(\alpha_0)Z(\alpha_0)/V$ is of the same size as the term $M_q(\alpha_0)F_\alpha^{(g)}/V$, but of different sign. (Therefore, the tail fin angle in Figure 3.15 which yields zero static aerodynamic pitch moment for the PGMM is the one that corresponds to $\hat{U}_0^{(y)}$ for glide.) Thus, by plotting $M_q(\alpha_0)Z(\alpha_0)/V$ as a function of α_0 (as in Figure 4.1) it is easy to estimate the size of the sum of these terms also for other values of α_0.

For maneuvering flight it is instructive to consider the gravity free case ($F_\alpha^{(g)} = 0$, $\dot{F}_\alpha^{(g)} = 0$), for example to assess horizontal turn performance (after a change to yaw plane variables). In this case the right hand side in (4.60) can be written

$$-M(\alpha_0,0) + M_q(\alpha_0)\frac{Z(\alpha_0)}{V},$$

which under the present linear approximation equals $-M(\alpha_0, q_0^{(a)})$. Thus, the right hand side gets a contribution only from the moment $M(\alpha_0, q_0^{(a)})$ at aerodynamic equilibrium and the trimming moment required for this flight case

is given by $-M(\alpha_0, q_0^{(a)})$. Finally, in the general case the right hand side of (4.60) is given (approximately) by (4.59), if we assume slowly varying gravity contribution ($\dot{F}_\alpha^{(g)} = 0$). Thus in this case the trim moment is simply $U_0^{(y,g)}$. If also the rightmost term on the right in (4.60) is to be included in the analysis of control effort it is perhaps best roughly estimated and then included in the allowable control error budget, see below.

4.4.2.1 Effects of nonstationary aerodynamics

It is common to include also instationary effects in the aerodynamics and the most prominent contributions are often those that depend on $\dot{\alpha}$. The discussion above is easy to generalize to incorporate also such effects, at least for the case where the normal force and pitch moment coefficients have linear dependence on $\dot{\alpha}$.

In case the right hand side of the α-dynamics in (4.45) contains a term which is linear in $\dot{\alpha}$ one can simply solve the resulting algebraic equation for $\dot{\alpha}$, which will again yield an equation of the form (4.45). Thus, after this substitution the expressions (4.53) and (4.54) will apply without change.

When the q-dynamics in (4.46) has a right hand side with linear dependence on $\dot{\alpha}$ then it is easy to see, by retracing the steps from (4.45) through (4.50) leading to (4.54), that the expression (4.54) will be replaced by

$$2\zeta_{sp}(\alpha_0)\omega_{sp}(\alpha_0) = -(M_q(\alpha_0) + M_{\dot{\alpha}}(\alpha_0) + Z_\alpha(\alpha_0)/V), \tag{4.61}$$

but the expression (4.53) will remain the same. The question then arises what the effects are of the term $M_{\dot{\alpha}}(\alpha_0)$ in (4.61).

To get some idea of this, at least for the PGMM, it is instructive to study the relative size of the terms making up the expression (4.61) given in Figure 4.1. From this figure it is clear that $Z_\alpha(\alpha_0)/V$ is clearly smaller in size than $M_q(\alpha_0)$, so a perturbation of $M_q(\alpha_0)$ with the term $M_{\dot{\alpha}}(\alpha_0)$ will likely not be "masked" by $Z_\alpha(\alpha_0)/V$ but will be visible in the result. At the same time we note that a perturbation of the term $M_q(\alpha_0)$ (due to e.g. an error) in (4.53) is not likely to have a large effect since the term $M_q(\alpha_0)Z_\alpha(\alpha_0)/V$ is, for angles of attack less than approximately 15°, much smaller than $M_\alpha(\alpha_0)$.

This means that the product $\zeta_{sp}(\alpha_0)\omega_{sp}(\alpha_0)$ will in fact be calculated more correctly if we use (e.g. inadvertently) a value for $M_q(\alpha_0)$ in (4.54) which in fact is a value for $M_q(\alpha_0) + M_{\dot{\alpha}}(\alpha_0)$, such as if we use the formula (3.22) which is based on the total body pitch damping contribution in (3.21). At the same time, doing the same substitution (e.g. inadvertently) in (4.53) when calculating $\omega_{sp}(\alpha_0)^2$ is likely to have little effect since the term $M_\alpha(\alpha_0)$ dominates $M_q(\alpha_0)Z_\alpha(\alpha_0)/V)$, at least for the PGMM as can be seen from Figure 4.1.

4.4.2.2 Short period dynamics of the PGMM

An example the resulting natural frequency $\omega_{sp}(\alpha_0)$ and damping $\zeta_{sp}(\alpha_0)$ as given by the short period approximation expressions in (4.53), (4.54) are shown in Figure 4.2 and in Figure 4.3 an example of how the pole locations vary with airspeed and angle of attack is given. From these figures it is clear that for the altitude $h = 1500$m and airspeed $V = 125$m/s the damping is low for angles of attack below 15°, in particular it is about 0.2 for coasting horizontal flight at approximately $\alpha = 9°$. There is also a fair amount of variation of the dynamics with the angle of attack and airspeed.

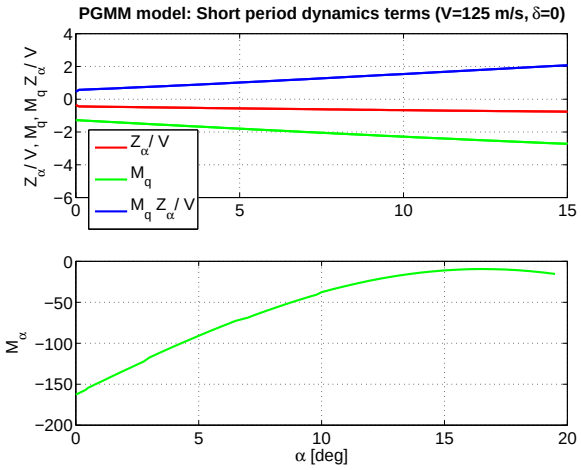

Figure 4.1: The different terms $Z_\alpha(\alpha_0)/V$, $M_q(\alpha_0)$, $M_q(\alpha_0)Z_\alpha(\alpha_0)/V$ (top) and $M_\alpha(\alpha_0)$ (bottom) that make up $\omega_{sp}(\alpha_0)$ and $\zeta_{sp}(\alpha_0)$ in (4.53), (4.54) for the PGMM as a function of angle of attack α_0, for the airspeed $V = 125$m/s and altitude $h = 1500$m. (The quantities in (4.53), (4.54) are defined for an aerodynamic equilibrium point $(\alpha_0, q_0^{(a)})$ as in (4.43), (4.44) but in the aerodynamic model of the PGMM there is no dependence on q_0 in these quantities.)

4.4.3 Normal force and normal acceleration

Normal acceleration is generally defined in E as $\boldsymbol{P}_{[\boldsymbol{V}]^\perp}\dot{\boldsymbol{V}}$, i.e. the component of the acceleration $\dot{\boldsymbol{V}}$ which is perpendicular to the velocity vector $\boldsymbol{V}$, and by

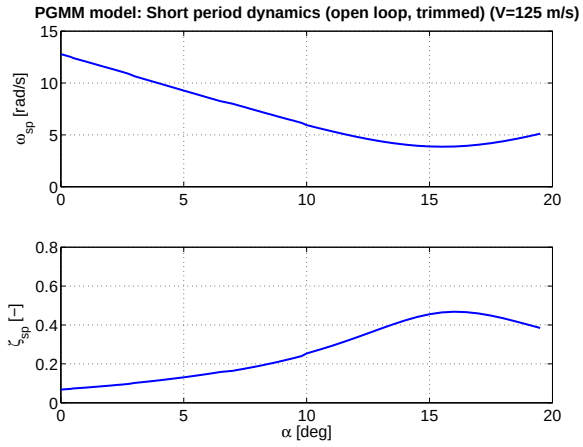

Figure 4.2: Natural frequency $\omega_{sp}(\alpha_0)$ (top) and damping $\zeta_{sp}(\alpha_0)$ (bottom) according to (4.53), (4.54) for the PGMM at as a function of angle of attack α_0, for the airspeed $V = 125$m/s and altitude $h = 1500$m. (There is no dependence on q_0 in ω_{sp}, ζ_{sp} for the PGMM model.)

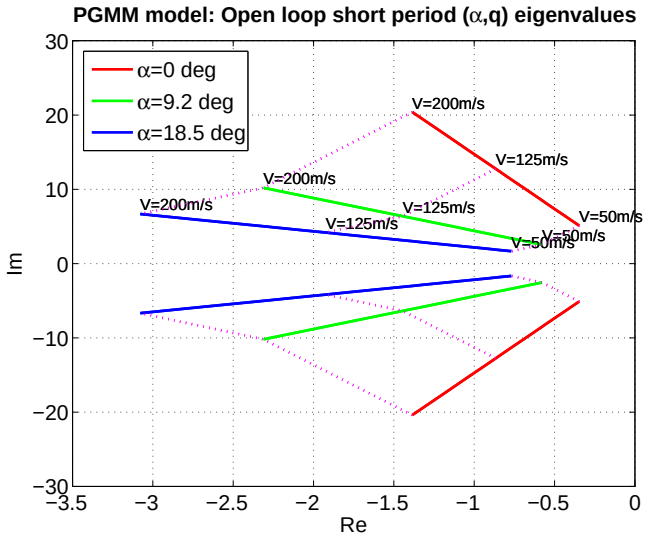

Figure 4.3: Variation in location of the poles $\lambda_{1,2} = -\zeta_{sp}\omega_{sp} \pm j\omega_{sp}\sqrt{1-\zeta_{sp}^2}$ in the complex plane for the short period approximation (4.53), (4.54) for the PGMM as a function of airspeed V and angle of attack α_0, at the altitude $h = 1500$m. (There is no dependence on q_0 in $\lambda_{1,2}$ for the PGMM model.)

(4.5), (4.7) and (4.8) it can be related to the force $\boldsymbol{f}$ in B as

$$\begin{aligned}
\boldsymbol{P}_{[\boldsymbol{V}]^\perp}\dot{\boldsymbol{V}} &= (\boldsymbol{I} - \boldsymbol{P}_{[\boldsymbol{V}]})\frac{1}{m}\boldsymbol{F} \\
&= \big(\boldsymbol{I} - \frac{1}{\|\boldsymbol{V}\|^2}\boldsymbol{V}\boldsymbol{V}^T\big)\frac{1}{m}\boldsymbol{R}(\boldsymbol{q})\boldsymbol{f} \\
&= \big(\boldsymbol{R}(\boldsymbol{q}) - \frac{1}{\|\boldsymbol{v}\|^2}\boldsymbol{R}(\boldsymbol{q})\boldsymbol{v}\boldsymbol{v}^T\big)\frac{1}{m}\boldsymbol{f} \\
&= \boldsymbol{R}(\boldsymbol{q})\big(\boldsymbol{I} - \boldsymbol{P}_{[\boldsymbol{v}]}\big)\frac{1}{m}\boldsymbol{f} \\
&= \boldsymbol{R}(\boldsymbol{q})\boldsymbol{P}_{[\boldsymbol{v}]^\perp}\frac{1}{m}\boldsymbol{f}, \qquad (4.62)
\end{aligned}$$

where we have used the fact that $\boldsymbol{R}(\boldsymbol{q})$ is a rotation matrix (and therefore orthogonal) several times. From (4.62) we see that it is natural to define normal acceleration in B simply as the term $\boldsymbol{P}_{[\boldsymbol{v}]^\perp}\boldsymbol{f}/m$, i.e. the projection of $\boldsymbol{f}/m$ onto the plane $[\boldsymbol{v}]^\perp$ perpendicular to the velocity vector $\boldsymbol{v}$ in B, and this is the definition we shall use. However, we are here going to focus on the aerodynamic contribution to (normalized) normal acceleration $\boldsymbol{P}_{[\boldsymbol{v}]^\perp}\boldsymbol{f}^{(a)}/(mg)$ in B, where the aerodynamic force vector $\boldsymbol{f}^{(a)}$ in B is defined in terms of the components in (4.4) as

$$\boldsymbol{f}^{(a)} = [f_x^{(a)}, f_y^{(a)}, f_z^{(a)}]^T.$$

In the xz-plane in B, the pitch plane, the (signed) magnitude of the aerodynamic normal acceleration η is defined in terms of the lift and weight force components f_L and f_W, respectively (cf. Section 3.3.2.1), as

$$\eta = \frac{f_L}{f_W} = \frac{f_L}{mg}. \qquad (4.63)$$

4.4.3.1 Pitch plane acceleration dynamics

For a missile which is symmetric with respect to mirroring in the xy-plane in B the lift force magnitude f_L is approximately proportional to α, for small α, cf. e.g. Figure 3.3. Therefore, also the deviation $\tilde{f}_L = f_L - f_{L_0}$ from the value f_{L_0} that corresponds to a reference value α_0 for the angle of attack is proportional to $\tilde{\alpha} = \alpha - \alpha_0$, for small deviations $\tilde{\alpha}$ (and small α_0). Since η is proportional to f_L it can be obtained (approximately) by a simple rescaling of α,

$$\eta = C_\eta \alpha, \tag{4.64}$$

cf. Figure 3.4. By comparing the expression for lift force f_L in terms of aerodynamic coefficients (3.4) with the definition of aerodynamic normal acceleration (4.63) we see that the scale factor C_η is given by

$$C_\eta = \frac{\rho V^2}{2mg} S_{ref} C_{L_\alpha}^{(0)},$$

where $C_{L_\alpha}^{(0)}$ denotes the lift coefficient derivative $C_{L_\alpha} = \partial C_L / \partial \alpha$ evaluated at 0.

A linear model for the acceleration dynamics expressed in terms of deviation $\tilde{\eta} = \eta - \eta_0$ from a reference value $\eta_0 = C_\eta \alpha_0$ can be directly obtained from the short period approximation (4.51) as

$$\ddot{\tilde{\eta}} + 2\zeta_{sp}\omega_{sp}\dot{\tilde{\eta}} + \omega_{sp}^2 \tilde{\eta} = \omega_{sp}^2(\tilde{\eta}_c + \eta^{(g)}), \tag{4.65}$$

where $\tilde{\eta}_c = \eta_c - \eta_0$ and the relations to the moments are given by[15]

$$\eta^{(g)} = \frac{C_\eta}{\omega_{sp}^2} U^{(g)}(\alpha_0), \quad \eta_c = \frac{C_\eta}{\omega_{sp}^2} U^{(y)}, \quad \eta_0 = \frac{C_\eta}{\omega_{sp}^2} U_0^{(y,a)}. \tag{4.66}$$

In this setting, the reference value for acceleration is η_0, the commanded value is η_c and the acceleration component $\eta^{(g)}$ which is due to acceleration enters as an auxiliary input. However, often it is convenient to lump the gravity component together with the reference value and rewrite the dynamics in terms of gravity compensated variables, in the sense discussed in Section 4.4.1.2.

To arrive at a gravity compensated form of the dynamics we define a new reference value $\hat{\eta}_0$ for the commanded acceleration as

$$\hat{\eta}_0 = \eta_0 - \eta^{(g)} \tag{4.67}$$

so that

$$\tilde{\eta}_c + \eta^{(g)} = \eta_c - (\eta_0 - \eta^{(g)}) = \eta_c - \hat{\eta}_0,$$

where

$$\hat{\eta}_0 = \frac{C_\eta}{\omega_{sp}^2} \hat{U}_0^{(y)} \tag{4.68}$$

and $\hat{U}_0^{(y)}$ is defined in (4.57). A new deviation variable $\nu = \eta_c - \hat{\eta}_0$ for the commanded acceleration can then be considered so that the dynamics (4.65) takes the form

$$\ddot{\tilde{\eta}} + 2\zeta_{sp}\omega_{sp}\dot{\tilde{\eta}} + \omega_{sp}^2 \tilde{\eta} = \omega_{sp}^2 \nu, \tag{4.69}$$

where $\nu = 0$ gives the aerodynamic normal acceleration η_0 for the aerodynamic equilibrium at α_0. Normally, the system (4.69) is operated with $\nu = 0$ since η_c

[15] With this scaling of $\tilde{\eta}_c + \eta^{(g)}$ the "gain" from $\tilde{\eta}_c + \eta^{(g)}$ to $\tilde{\eta}$ becomes 1 in steady state.

is chosen to track changes in $\hat{\eta}_0$ which then, in effect, becomes the commanded variable.

The representation (4.69) is very useful for performance modeling since it *contains all the essential features of the linearized pitch plane aerodynamic acceleration dynamics, while suppressing the less important ones* (such as exactly how the input is formed from (supposedly) known quantities).

A state space realization of the dynamics (4.65), or the gravity compensated form (4.69), is immediately obtained from (4.55) and (4.66), or (4.67).

4.4.4 Drag force

So far we have concentrated on developing a simplified, but still relatively detailed, model of forces (accelerations) in the normal direction (i.e. perpendicular to the velocity vector $\boldsymbol{v}$) in the xz-plane in B. What remains to get the pitch plane dynamics model complete is expressions for forces (accelerations) parallel to the velocity vector. Since it is straightforward to add a force representing the thrust (i.e. thrust force components in the normal direction and its orthogonal complement), and since the PGMM lacks propulsion, we shall here only consider the non-powered case so that the force component in the pitch plane parallel to the velocity vector is the drag f_D only (cf. Section 3.4).

From (4.17) we know that the change in airspeed $\dot{V}$ is determined by the force component parallel to the velocity vector $\boldsymbol{v}$, which in the pitch plane representation (for non-powered flight) is f_D, but we have not discussed here how this force can be related to the other variables in the pitch plane dynamics. However, from Section 3.4 we know that f_D can be decomposed into two components as $f_D = f_{D0} + f_{Di}$ where the base drag f_{D0} is independent of α and the induced drag f_{Di} is approximatively proportional to α^2. Since f_{Di} is approximately proportional to α^2 is it approximatively proportional to the lift force f_L, cf. Figure 4.4, and can thus be expressed as a (linear) function of f_L, or (by using (4.64)) as a linear function of the aerodynamic normal acceleration η.

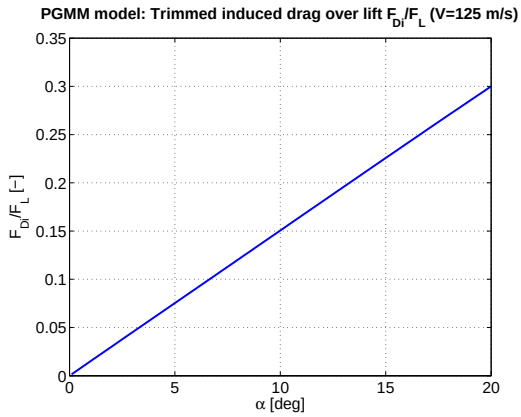

Figure 4.4: Ratio of induced drag force f_{Di} over lift force f_L as a function of angle of attack α for the PGMM at the airspeed $V = 125$m/s and altitude $h = 1500$m.

4.5 Controller

4.5.1 Synthesis of normal acceleration dynamics

The expression (4.69) above describes the open loop (no controller) system dynamics for the aerodynamic contribution to normal acceleration (deviation) $\tilde{\eta}$ in the pitch plane, where commanded normal acceleration η_c is the control variable for variations around a reference value $\hat{\eta}_0$ (which corresponds to an angle of attack α_0, at a given orientation of the missile since gravity is included in the reference value). Due to the variation in these dynamics with the flight condition which is common, cf. Figure 4.3, a controller is normally placed between these dynamics and the guidance system, and this controller (*autopilot* in missile parlance) synthesizes desired dynamics for the normal acceleration (from commanded normal acceleration η_c) to actual ditto $\tilde{\eta}$. By a remark made in connection with (4.69) we know that this is normally by be interpreted as the dynamics for regulation of the system (4.69) around a reference value of $\nu = 0$.

Simple missiles do not have sensors to directly measure the angle of attack α but often have sensors to measure accelerations and angular accelerations (such as $\dot{q}, \dot{r}$), and hence also (via integration) q, r and the orientation of the gravity vector in the body system B. This, together with the simple linear relation (4.46) which relates $\tilde{q}, \dot{\tilde{q}}, \tilde{\alpha}$ and the deviation $\tilde{U}$ from reference in the moment makes it reasonable to assume that also $\tilde{\alpha}$ is available[16] for feedback, and via (4.45) also $\dot{\tilde{\alpha}}$. One can therefore assume that $\tilde{\alpha}, \tilde{q}$ are available for state feedback, alternatively $\tilde{\alpha}, \dot{\tilde{\alpha}}$, also for many simpler missiles. For these reasons we shall employ state feedback (using the full state vector) in the synthesis of pitch plane dynamics.

4.5.1.1 Pole placement

To see how linear pitch plane dynamics synthesis can be realized we assume that we have some given desired (aerodynamic) normal acceleration dynamics, e.g. in terms of deviation variables (with gravity compensation) as

$$\ddot{\tilde{\eta}} + 2\zeta_{sp,d}\omega_{sp,d}\dot{\tilde{\eta}} + \omega_{sp,d}^2\tilde{\eta} = \omega_{sp,d}^2\hat{\nu}, \tag{4.70}$$

where $\omega_{sp,d}$ and $\zeta_{sp,d}$ are desired values for the natural angular frequency and damping, respectively, and $\hat{\nu}$ is a new input variable (see below). If we then let the commanded acceleration η_c in (4.69) be given as $\eta_c = \hat{\eta}_c$ where $\hat{\eta}_c$ is a linear (affine) function of $\tilde{\eta}, \dot{\tilde{\eta}}$ as

$$\hat{\eta}_c = \hat{\eta}_0 + k_0\tilde{\eta} + k_1\dot{\tilde{\eta}} + c\hat{\nu}, \tag{4.71}$$

where k_0, k_1, c are three constants, and compare with (4.70) we see that if we choose

$$\begin{aligned} k_0 &= (\omega_{sp}^2 - \omega_{sp,d}^2)/\omega_{sp}^2, \\ k_1 &= 2(\zeta_{sp}\omega_{sp} - \zeta_{sp,d}\omega_{sp,d})/\omega_{sp}^2, \\ c &= \omega_{sp,d}^2/\omega_{sp}^2, \end{aligned} \tag{4.72}$$

then the desired dynamics is realized for the closed loop system. Again, the value for the input variable $\hat{\nu}$ which ought to be the most common is 0 since the acceleration command is implicitly communicated to the system through the (gravity compensated) reference value $\hat{\eta}_0$.

[16] In practice several of the aerodynamic derivatives, which are required in order to calculate $\alpha, \dot{\alpha}$, are not known exactly and different forms of observers or estimators are used to estimate $\alpha, \dot{\alpha}$.

A state space realization of the simple (gravity compensating) pole placement controller (4.71) and (4.72) is readily obtained from (4.55) and (4.64).

4.5.2 Control authority for dynamics synthesis

To synthesize the desired dynamics (4.70) for deviations around (a gravity compensated) reference value $\hat{\eta}_0$ (i.e. in practice to "bring back" η to $\hat{\eta}_0$ after a change in the latter) requires further moments than those corresponding to $\hat{U}_0^{(y)}$ in (4.60), and these additional moments are in the worst case determined by the maximally allowed values of $\tilde{\eta}, \dot{\tilde{\eta}}$, or equivalently, the maximally allowed values of $\tilde{\alpha}, \dot{\tilde{\alpha}}$.

To see how large the additional moments can be we note that when controlling the (aerodynamic) normal acceleration η around a reference value $\hat{\eta}_0$ with the controller in (4.71) the variable $\hat{\nu}$ in (4.70) is identically zero and we get the following bound for the deviation $\hat{\eta}_c - \hat{\eta}_0$ between commanded normal acceleration and the reference value for acceleration commands

$$\begin{aligned} |\hat{\eta}_c - \hat{\eta}_0| &= |k_0\tilde{\eta} + k_1\dot{\tilde{\eta}}| \\ &\leq |k_0||\tilde{\eta}|_{max} + |k_1||\dot{\tilde{\eta}}|_{max} \\ &= C_\eta(|k_0||\tilde{\alpha}|_{max} + |k_1||\dot{\tilde{\alpha}}|_{max}), \end{aligned} \tag{4.73}$$

where the max-limits $|\tilde{\alpha}|_{max}, |\dot{\tilde{\alpha}}|_{max}$ for $\tilde{\alpha}, \dot{\tilde{\alpha}}$, respectively, are given by structural or aerodynamic limitations, or limitations in the actuators. Since $\hat{\eta}_c$ is simply a value for the command η_c issued by the controller (4.71) we can use (4.66) and (4.68) to obtain the following relation between deviation in acceleration variables and deviation in normalized control moments

$$U^{(y)} - \hat{U}_0^{(y)} = \frac{\omega_{sp}^2}{C_\eta}(\hat{\eta}_c - \hat{\eta}_0), \tag{4.74}$$

where the value $U^{(y)} = \hat{U}_0^{(y)}$ of the normalized control surface induced moment yields the aerodynamic equilibrium $(\alpha_0, q_0^{(a)})$ for the dynamics in (4.55), (4.56). Therefore, if we define the reference moment $\hat{u}_{y,0}$ by

$$\hat{u}_{y,0} = J_{yy}\hat{U}_0^{(y)} \tag{4.75}$$

and recall (from (4.35)) that $u_y = J_{yy}U^{(y)}$ we obtain from (4.73) and (4.74) for the deviation moment $u_y - \hat{u}_{y,0}$ corresponding to $\hat{\eta}_c - \hat{\eta}_0$ the following estimate

$$\begin{aligned} \frac{|u_y - \hat{u}_{y,0}|}{J_{yy}} &= |U^{(y)} - \hat{U}_0^{(y)}| \\ &= \frac{\omega_{sp}^2|\hat{\eta}_c - \hat{\eta}_0|}{C_\eta} \\ &\leq \omega_{sp}^2(|k_0||\tilde{\alpha}|_{max} + |k_1||\dot{\tilde{\alpha}}|_{max}) \\ &= |\omega_{sp}^2 - \omega_{sp,d}^2||\tilde{\alpha}|_{max} + 2|\zeta_{sp}\omega_{sp} - \zeta_{sp,d}\omega_{sp,d}||\dot{\tilde{\alpha}}|_{max}, \end{aligned}$$

with k_0, k_1 given by (4.72). It follows that the control surface induced moment u_y can be bounded as follows

$$\begin{aligned} u_y &\leq \hat{u}_{y,0} + J_{yy}(|\omega_{sp}^2 - \omega_{sp,d}^2||\tilde{\alpha}|_{max} + 2|\zeta_{sp}\omega_{sp} - \zeta_{sp,d}\omega_{sp,d}||\dot{\tilde{\alpha}}|_{max}), \\ u_y &\geq \hat{u}_{y,0} - J_{yy}(|\omega_{sp}^2 - \omega_{sp,d}^2||\tilde{\alpha}|_{max} + 2|\zeta_{sp}\omega_{sp} - \zeta_{sp,d}\omega_{sp,d}||\dot{\tilde{\alpha}}|_{max}). \end{aligned} \tag{4.76}$$

We remark that even though the bounds in (4.76) apply to the case where the reference moment $\hat{u}_{y,0}$ as in (4.75) is nonzero, the most interesting case (for a missile which is symmetric with respect to mirroring in the xy-plane) to apply the bound (4.76) on ought to be when $\alpha_0 = 0$ so that $\hat{u}_{y,0} = 0$.

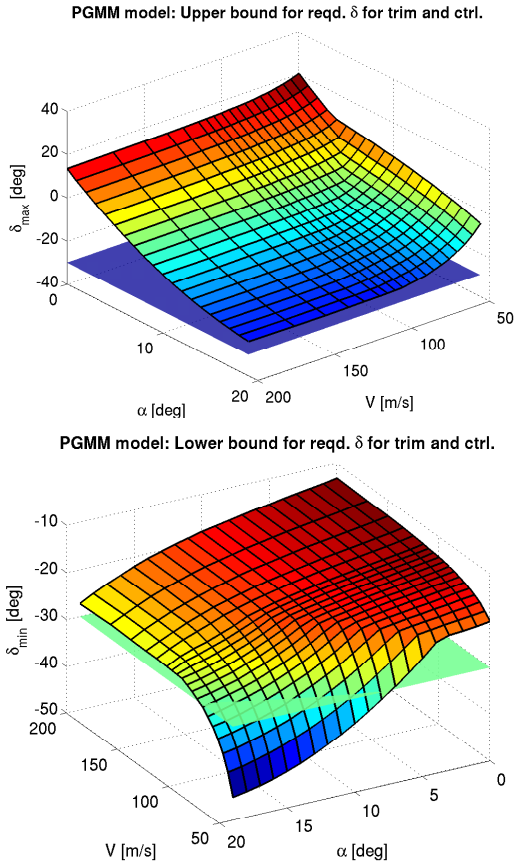

Figure 4.5: The resulting upper bound (top) and lower bound (bottom) for the tail fin deflection δ of the PGMM based on the bounds (4.76) and the values for $\zeta_{sp,d}$, $\omega_{sp,d}$, $|\tilde{\alpha}|_{max}$ and $|\dot{\tilde{\alpha}}|_{max}$ in (4.77), for gravity free flight operation around an aerodynamic equilibrium point, at the airspeed $V = 125$m/s and altitude $h = 1500$m. The lower limit $\delta = -30^\circ$ for control surface deflection is indicated by a plane in both panels.

4.5.3 Required control effort for the PGMM

An example of the bound (4.76) for the PGMM computed with the values

$$\begin{array}{rcl} \zeta_{sp,d} & = & 0.7, \\ \omega_{sp,d} & = & 4\text{rad/s}, \\ |\tilde{\alpha}|_{max} & = & 0.25\text{rad} \approx 15^\circ, \\ |\dot{\tilde{\alpha}}|_{max} & = & 1.5\text{rad/s} \approx 90^\circ/\text{s} \end{array} \tag{4.77}$$

and translated to total control surface (tail fin) deflection δ is given in Figures 4.5 and 4.6. The value for the reference moment $\hat{u}_0$ as in (4.75) is taken from the expression (4.60) but without gravity effects ($F_\alpha^{(g)} = 0$, $\dot{F}_\alpha^{(g)} = 0$) and for a reference point (α_0, q_0) which corresponds to aerodynamic equilibrium as in (4.43), (4.44). It is clear that the desired dynamics can be synthesized for a large domain of values of α_0, V since the required control surface deflections δ are well within $\pm 30^\circ$, except for the very lowest airspeeds where the limit $\delta = -30^\circ$ is crossed.

From Figures 4.5 and 4.6 it is evident that the major contributing factor

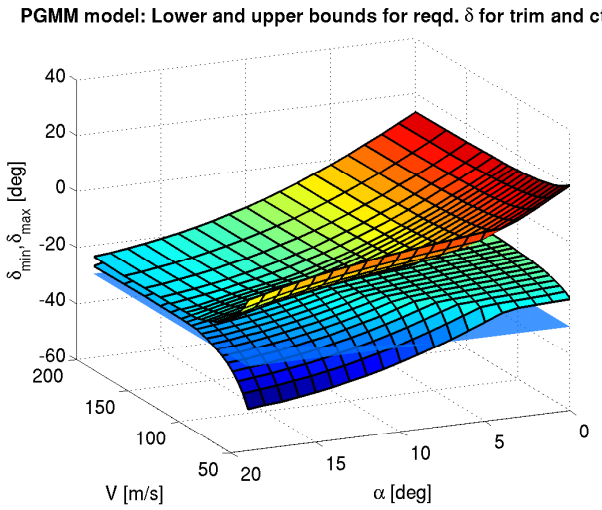

Figure 4.6: Same data as in Figure 4.5, but combined in one panel. The lower limit $\delta = -30°$ for control surface deflection is indicated by a plane.

to large values of the required control surface moments $|u_y|$ in (4.76), and corresponding deflections, is the low efficiency of the control surfaces at low dynamic pressures, i.e. low airspeeds. The low damping of the (open loop) short period dynamics at low angles of attack also requires some control effort to remove with the dynamics synthesis, with increased requirements on the control surface deflections as a result.

4.6 Total (Simplified) Model

We now have all the components required to assemble a simplified model of the total missile dynamics. In the following we shall briefly discuss how this can be done in an implementation for simulation. The total model will be of the "2+3" degree-of-freedom form discussed in Section 1.2 with 11 or 12 states, depending on the representation of the orientation, and the base will be the simplified (and decoupled) models for the pitch and yaw planes obtained via the short period approximation derived and discussed in Section 4.4. The reader is reminded that we consider only non-powered flight but the addition of thrust to the model is straightforward (mathematically, it will have the same effect as modifying one or several of the gravity force components in the body equations).

4.6.1 General structure

The most fundamental part of the overall dynamical model of the missile is Newton's second law (4.7) for the center-of-mass in E. We know from (4.8) that the force $\boldsymbol{F}$ in E is given by $\boldsymbol{F} = \boldsymbol{R}(\boldsymbol{q})\boldsymbol{f}$, where $\boldsymbol{R}(\boldsymbol{q})$ is the rotation matrix in (4.5), and that we can partition the force as $\boldsymbol{F} = \boldsymbol{F}^{(a)} + \boldsymbol{F}^{(g)}$ where

$$\boldsymbol{F}^{(a)} = \boldsymbol{R}(\boldsymbol{q})\boldsymbol{f}^{(a)}, \quad \boldsymbol{F}^{(g)} = \boldsymbol{R}(\boldsymbol{q})\boldsymbol{f}^{(g)}, \tag{4.78}$$

with aerodynamic and gravity induced components, respectively, according to

$$\boldsymbol{f}^{(a)} = [f_x^{(a)}, f_y^{(a)}, f_z^{(a)}]^T, \quad \boldsymbol{f}^{(g)} = [f_x^{(g)}, f_y^{(g)}, f_z^{(g)}]^T.$$

The force component $\boldsymbol{P}_{[\boldsymbol{v}]^\perp}\boldsymbol{f}^{(a)}$ is the aerodynamic normal force (the lift force) in B and from Section 3.3 we know that it is (primarily) dependent on the aerodynamic angles α, β (although only the pitch plane lift force was studied there, which we modeled to have dependence on only α). In Sections 4.3 and 4.4 we developed a simplified model of the dynamics of the missile where the state variables are the aerodynamic angles α, β and the angular rates q, r (and, again, we focussed on the pitch plane, relying on symmetry to obtain the corresponding relations for the yaw plane). In this model, the aerodynamic force $\boldsymbol{f}^{(a)}$, the aerodynamic moments $\boldsymbol{m}^{(a)} + \boldsymbol{u}$ and the gravitation force $\boldsymbol{f}^{(g)}$ can be interpreted as driving terms, and the airspeed V is a parameter. (Moreover, we showed in Section 4.5 that the structure of the simplified model remains after addition of a linear state feedback controller.) For the evolution of V we have the basic relation (4.17).

Together this outlines a fairly complete model; what remains is dynamic relations for the orientation angles of B relative to E (which are needed to determine $\boldsymbol{f}^{(g)}$) and relations to translate the velocities (4.10)–(4.12) in B into velocities in E, and eventually, locations in E. In the following we shall describe how this model can be completed, and comment on some implementation aspects and the choices related to it.

4.6.2 Pitch plane

The aerodynamic normal force $\boldsymbol{P}_{[\boldsymbol{v}]^\perp}\boldsymbol{f}^{(a)}$ is, when projected onto the xz-plane, approximately (for small α, β) equal to the pitch plane lift force f_L. From Section 3.3 we know that f_L is roughly proportional to the angle of attack α. In Section 4.4 we have developed linear dynamic relations (the short period approximation etc.) for how α (and q) evolves over time, where the pitch plane representations of the aerodynamic forces and gravity act as driving terms and the airspeed V is a parameter. In these relations, the drag force f_D does not enter but f_D is necessary to know in order to determine the evolution of V.

From Section 3.4 we know that the drag f_D is quadratic in α (with no linear term), where the second degree term f_{Di} of f_D is essentially linear in f_L. Put together this results in a pitch plane model where, in terms of deviation variables, the commanded angle of attack (or, equivalently, the aerodynamic normal force) defines an input to a second order linear dynamic system in the variable $\tilde{\alpha} = \alpha - \alpha_0$ with outputs $\tilde{f}_L = f_L - f_{L_0}$ and $\tilde{q} = q - q_0$, and the drag component f_D is obtained as a nonlinear function of $\tilde{\alpha}$ (since f_D is quadratic in $\alpha = \tilde{\alpha} + \alpha_0$ where α_0 can be regarded as a parameter). A block diagram over this dynamic system is given in Figure 4.7.

4.6.3 Pitch and yaw planes

We know that by complementing the pitch plane model described above for the dynamics of α, q with an analogous model for the dynamics of β, r we obtain a linearized model for the longitudinal and lateral dynamics in body coordinates (where the assumption $p = 0$ is implicit). We also have a dynamical relation for how the airspeed V is evolving over in (4.17), where the driving term F_V is the component of the force $\boldsymbol{f}^{(a)} + \boldsymbol{f}^{(g)}$ in B which lies in $[\boldsymbol{v}]$. To employ the relation (4.17) for V correctly we have to exercise some care, however, since the the drag in B, which is given by the term $\boldsymbol{P}_{[\boldsymbol{v}]}\boldsymbol{f}^{(a)}$, has a quadratic dependence on both α, β (cf. Section 3.4), i.e. total angle of attack α_t must be used. Hence, when calculating the evolution of V in a full model we must use data from the pitch and yaw planes simultaneously.

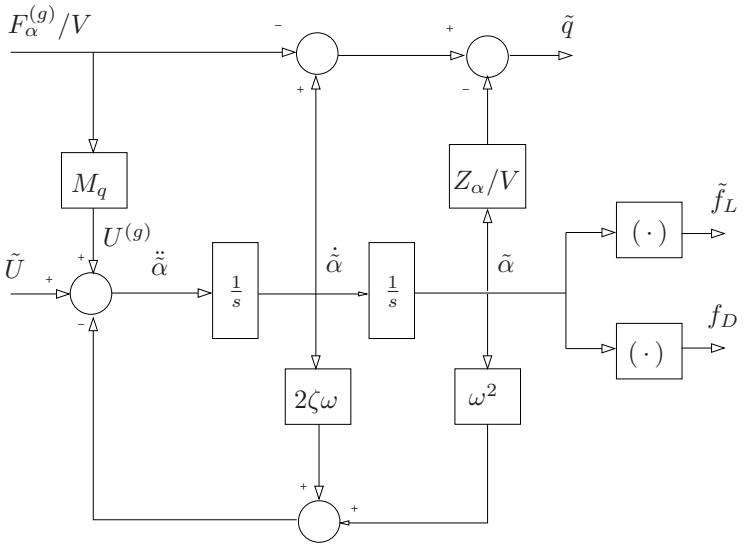

Figure 4.7: Block diagram over the structure in the simplified missile dynamics in the pitch plane based on linearization and slowly changing gravity contribution. Deviation variables are used; the reference values α_0, q_0, U_0 correspond to aerodynamic force and moment equilibrium (4.43), (4.44), and the value for the corresponding lift force f_{L_0} is taken from a table, such as e.g. Figure 3.3. The deviation in lift force $\tilde{f}_L$ is linear in $\tilde{\alpha}$ and the drag f_D is quadratic in α, where one part is constant and one part is linear in $\tilde{f}_L$; also these parts are taken from tables such as Figure 4.4. In the overall model there is moreover a parametric dependence on the reference value α_0, the airspeed (which is modeled separately, cf. (4.15), (4.17)) and the orientation of the missile and the altitude. If the drag f_D is not of interest (and therefore can be disregarded) the gravity term $F_\alpha^{(g)}$ can be set to zero here and gravity is added separately via $\boldsymbol{F}^{(g)}$ in E instead (since the map $(F_\alpha^{(g)}, \tilde{U}) \mapsto (\tilde{f}_L, \tilde{q})$ is linear).

4.6.4 Representation in aerodynamic coordinates

If we use the state space representation (4.55) for the linearized pitch plane dynamics, and a similar representation for the dynamics in the yaw plane, then both the open and closed loop system dynamics[17] for the missile together with the orientation relation (4.6) can be written on state space form as

$$\dot{\boldsymbol{q}} = \frac{1}{2}\boldsymbol{q} \circ (0, \boldsymbol{\omega}(\tilde{\boldsymbol{x}}, \boldsymbol{\theta})), \tag{4.79}$$

$$\dot{V} = D(V, \tilde{\boldsymbol{x}}, \boldsymbol{\theta}), \tag{4.80}$$

$$\dot{\tilde{\boldsymbol{x}}} = \boldsymbol{A}(V, \boldsymbol{\theta})\tilde{\boldsymbol{x}} + \boldsymbol{B}(\boldsymbol{u}_g(\boldsymbol{q}, V, \tilde{\boldsymbol{x}}, \boldsymbol{\theta}) + \tilde{\boldsymbol{u}}_c), \tag{4.81}$$

where $\tilde{\boldsymbol{x}} = [\tilde{\alpha}, \dot{\tilde{\alpha}}, \tilde{\beta}, \dot{\tilde{\beta}}]^T$, $\boldsymbol{\omega}(\tilde{\boldsymbol{x}}, \boldsymbol{\theta}) = [p, q, r]^T$ (where $p \equiv 0$) with q, r obtained from (4.45) and its yaw plane equivalent. (Alternatively, one can of course use the state vector $[q, \alpha, r, \beta]^T$ and (4.47), which in practice might be preferable since (at least) the angular rates q, r are in general directly measurable via onboard sensors.) The vector $\boldsymbol{\theta}$ contains all quantities which can be regarded as

[17] From the discussion in Sect 4.5.1 we know that the closed loop system in the pitch and yaw planes will have the same form as the open loop system and if the dynamics synthesis by the controller is capable of realizing constant dynamics then the matrix $\boldsymbol{A}(V, \boldsymbol{\theta})$ becomes independent of $V, \boldsymbol{\theta}$.

"parameters" here, such as the reference values $\alpha_0, q_0, \beta_0, r_0$ and the altitude h, and the equation (4.80) represents the equation (4.17) for the airspeed V. The two two-dimensional input signals to the four-dimensional linear system (4.81) are the vector $\tilde{\boldsymbol{u}}_c$ of commanded deviations from the reference values for the moments in the pitch and yaw planes, respectively, as in (4.56), and the vector $\boldsymbol{u}_g(\boldsymbol{q}, V, \tilde{\boldsymbol{x}}, \boldsymbol{\theta})$ which represents the corresponding gravity induced contributions in the two planes. The 4×4-dimensional matrix $\boldsymbol{A}(V, \boldsymbol{\theta})$ is block diagonal, since the pitch and yaw channel dynamics are decoupled after linearization, and the 4×2-dimensional matrix $\boldsymbol{B}$ has a corresponding block structure. Since $\dot{\boldsymbol{F}}^{(g)} = 0$ we have

$$\dot{\boldsymbol{f}}^{(g)} = \dot{\boldsymbol{R}}(\boldsymbol{q})^T \boldsymbol{F}^{(g)} = \dot{\boldsymbol{R}}(\boldsymbol{q})^T \boldsymbol{R}(\boldsymbol{q}) \boldsymbol{f}^{(g)} = \boldsymbol{\omega}(\tilde{\boldsymbol{x}}, \boldsymbol{\theta}) \times \boldsymbol{f}^{(g)}.$$

This means that if we use the approximation (for small angles α, β and small axial force f_x, cf. Section 4.3.2)

$$\frac{d}{dt}\frac{F_\alpha^{(g)}}{V} = \frac{d}{dt}\frac{f_z^{(g)}}{mV} \tag{4.82}$$

we have

$$\frac{d}{dt}\frac{F_\alpha^{(g)}}{V} = \frac{\dot{f}_z^{(g)}}{mV} - \frac{f_z^{(g)}\dot{V}}{mV^2} = \frac{\dot{f}_z^{(g)}}{mV} - \frac{F_\alpha^{(g)} D(V, \tilde{\boldsymbol{x}}, \boldsymbol{\theta})}{V^2},$$

and similarly for $(d/dt)(F_\beta^{(g)}/V)$, so that the components of $\boldsymbol{u}_g(\boldsymbol{q}, V, \tilde{x}, \theta)$ can be expressed solely with the aid of the state space variables in (4.79)–(4.81) and the gravity vector components, as alluded to above.

The solution to the equations (4.79)–(4.81) provide the orientation of the missile and the velocity vector in the body fixed system B, and to obtain the location of the missile in the Earth fixed system E one needs additional equations. A natural approach to obtain this is to simply rotate the velocity vector components to the Earth fixed system and thus obtain a system which after one integration gives the desired locations. One then adds the following equations to the model,

$$\dot{\boldsymbol{X}} = \boldsymbol{R}(\boldsymbol{q}) \boldsymbol{v}(\boldsymbol{q}, V, \tilde{\boldsymbol{x}}, \boldsymbol{\theta}). \tag{4.83}$$

The total model (4.79)–(4.83) has 12, or 11 states if e.g. Euler angles are used instead of the quaternion in (4.79) (alternatively, the redundancy in (4.79) is exploited in some other way).[18]

4.6.5 Further simplifications

It is desirable to investigate what further simplifications can be made in the total dynamics in (4.79)–(4.83). To begin with we can use the same approximation as in (4.82) and neglect the dependence on α, β in $F_\alpha^{(g)}, F_\beta^{(g)}$ which gives

$$\boldsymbol{u}_g(\boldsymbol{q}, V, \tilde{\boldsymbol{x}}, \boldsymbol{\theta}) = \boldsymbol{u}_g(\boldsymbol{q}, V, 0, \boldsymbol{\theta}).$$

Further, during (at least moderate) maneuvering the term $\boldsymbol{u}_g(\boldsymbol{q}, V, 0, \boldsymbol{\theta})$ can be considerably smaller than $\tilde{\boldsymbol{u}}_c$ and therefore one can then approximatively set $\boldsymbol{u}_g(\boldsymbol{q}, V, 0, \boldsymbol{\theta}) = 0$ in (4.81). (For the PGMM this is not the case however, since it has only small maneuvering capabilities, in the order of a few g's.)

One can of course also substitute the state space representation (4.55) which is part of (4.81) with (4.47), and proceed correspondingly for those parts of

[18] This is one more state variable than the minimal number 10 required, as described in a footnote in the Introduction.

(4.81) which describe the dynamics in the yaw plane. By doing so one gets rid of the term $\dot{F}_{\alpha}^{(g)}$ which is part of $\boldsymbol{u}_g(\boldsymbol{q}, V, 0, \theta)$, and a corresponding term for the yaw plane, but will then instead have the problem of expressing the closed loop system dynamics in terms of a mix of the aerodynamic quantities which are part of (4.47) and feedback terms, instead of only generic natural frequency and damping terms as in (the second row in) (4.55).

4.6.6 Acceleration variables

By applying the linear transformation (4.64) to the components in the vector $\tilde{\boldsymbol{x}}$ the total dynamics in (4.79)–(4.81) can be obtained on acceleration form.

Bibliography

Abney, E. & McDaniel, M. 2005 High angle of attack aerodynamic predictions using missile datcom. In *Proc. 23:rd AIAA Applied Aerodynamics Conference*. Toronto, Ontario Canada. AIAA paper 2005-5086.

A.E. Bryson, J. 1953 Stability derivatives for a slender missile with application to a wing-body-vertical-tail configuration. *Journal of the Aeronautical Sciences*, **20**(5), 297–308.

Aiello, G. & Bateman, M. 1979 Aerodynamic stability technology for maneuverable missiles, vol. 1. configuration aerodynamic characteristics. Technical Report AFFDL-TR-76-55, vol. 1, U.S. Airforce Flight Dynamics Laboratory, Wright Patterson Air Force Base, Dayton, OH.

Ananthkrishnan, N. & Unnikrishnan, S. 2001 Literal approximations to aircraft dynamic modes. *J. Guidance, Control and Dynamics*, **24**(6), 1196–1203.

Bischer, G. 1999 Precision guided mortar munition. Presentation available at `http://www.dtic.mil/ndia/infantry` (retrieved Oct. 2008).

Blakelock, J. 1991 *Automatic Control of Aircraft and Missiles*. Wiley, New York, NY, 2nd edition.

Blundell, M. & Harty, D. 2004 *The Multibody Systems Approach to Vehicle Dynamics*. Elsevier, Oxford, UK.

Boiffier, J.-L. 1998 *The Dynamics of Flight - The Equations*. Wiley, New York, NY.

Fleeman, E. L. 2006 *Tactical Missile Design*. Education Series. AIAA, Reston, VA, 2nd edition.

Hollingsworth, L. 2002 PGMM XM395 precision guided mortar munition. In *Proc. 7:th Intl. Artillery and Indirect Fire Symposium & Exhibition*. Presentation available at `http://www.dtic.mil/ndia/2002artillery` (retrieved Oct. 2008).

Jerger, J. 1960 *Systems Preliminary Design, Principles of Guided Missile Design*. Van Nostrand, Princeton, NJ.

Johansson, H. 1998 Mathematical modeling and simulation of a missile. Technical Report FOA-R–98-00876-314–SE, Swedish Defence Research Establishment, FOA.

Jorgensen, L. 1973 Prediction of static aerodynamic characteristics for space-shuttle-like and other bodies at angles of attack from 0° to 180°. Technical Report TN D-6996, NASA Ames Research Center, CA.

Kane, T. & Lewinson, D. 1985 *Dynamics: Theory and Applications*. Series in Mechanical Engineering. McGraw-Hill, New York, NY.

Kane, T. & Wang, C. 1965 On the derivation of equationsof motion. *J. of the Society of Industrial and Applied Mathematics*, **13**(2), 487–492.

Karnopp, D. 2004 *Vehicle Stability*. Marcel Dekker, New York, NY.

Khalil, H. 2002 *Nonlinear Systems*. Prentice Hall, Upper Saddle River, NJ, 3rd edition.

Lesieutre, D., Love, J. & Dillenius, M. 1996 High angle of attack missile aerodynamics including rotational rates - Program M3HAX. In *Proc. Atmospheric Flight Mechanics Conference*. San Diego, CA. AIAA paper 96-3392.

Ness, L. (Editor) 2004 *Jane's Ammunition Handbook 2004-2005*. Jane's Information Group, Coulsdon, Surrey, UK, 13th edition.

Pamadi, B. N. 2004 *Performance, Stability, Dynamics and Control of Airplanes*. Education Series. AIAA, Reston, VA, 2nd edition.

Pierens, D. 1994 Pitch and roll damping coefficients of the australian 81-mm improved mortar projectile. Technical Report DSTO-TR-0020, Aeronautical and Maritime Research Laboratory, Melbourne, Australia.

Pitts, W., Nielsen, J. & Kaattari, G. 1957 Lift and center of pressure of wing-body-tain combinations at subsonic, transonic and supersonic speeds. Technical Report NACA-1307, National Advisory Comittee for Aeronautics.

Sacks, A. 1954 Aerodynamic forces, moments, and stability derivatives for slender bodies of general cross section. Technical Report NACA-TN-3283, National Advisory Council for Aeronautics, Moffett Field, CA.

Simon, J. M. & Blake, W. B. 1999 Missile DATCOM: high angle of attack capabilities. In *Proc. AIAA Atmospheric Flight Mechanics Conference and Exhibit*. Portland, OR. AIAA paper 99-4258.

Sooy, T. & Schmidt, R. 2005 Aerodynamic predictions, comparisons, and validations using missile DATCOM (97) and aeroprediction 98 (AP98). *J. Spacecraft and Rockets*, **42**(2).

Standard Atmosphere 1975 International organization for standardization. ISO 2533:1975.

Stevens, B. & Lewis, F. 2003 *Aircraft Control and Simulation*. John Wiley & Sons, Inc., New York, NY, 2nd edition.

Tavares, T. 1990 *Aerodynamics of Maneuvering Slender Wings with Leading-Edge Separation*. Ph.D. thesis, Massachusetts Inst. Technol.

Weinacht, P. & Danberg, J. 2004 Prediction of the pitch-damping coefficients using sack's relations. Technical Report ARL-TR-3231, U.S. Army Research Laboratory, Aberdeen Proving Ground, MD.

Weinacht, P. & Danberg, J. 2005 Prediction of the pitch-damping coefficients using sacks's relations. *Journal of Spacecraft and Rockets*, **42**(5), 865–872.

Zarchan, P. 1994 *Tactical and Strategic Missile Guidance*, volume 157 of *Progress in Aeronautics and Astronautics*. AIAA.